PACIFIC EARTHQUAKE ENGINEERING
RESEARCH CENTER

Probabilistic Response Assessment for Building-Specific Loss Estimation

Eduardo Miranda
Stanford University

and

Hesameddin Aslani
Stanford University

PEER 2003/03
SEPT. 2003

Probabilistic Response Assessment for Building-Specific Loss Estimation

Eduardo Miranda
Structural Engineering and Geomechanics Division
Dept. of Civil and Environmental Engineering
Stanford University

Hesameddin Aslani
Graduate Student Researcher
Stanford University

PEER Report 2003/03
Pacific Earthquake Engineering Research Center
College of Engineering
University of California Berkeley
September 2003

ABSTRACT

The use of economic losses as measure of seismic performance is proposed. A methodology is developed to evaluate the expected annual loss in buildings resulting from the occurrence of earthquake ground motions. The methodology uses a component-based approach to estimate the expected loss in buildings.

A primary step in building loss estimation is a probabilistic evaluation of the structural response. A procedure aimed at computing the probability of exceedance of different types of engineering demand parameters (*EDPs*) is proposed. Emphasis is given to the estimation of the probability of exceedance of peak interstory drifts and peak floor accelerations at all levels in buildings. The peak interstory drift ratio at each story provides a way to estimate the damage to structural components and some of the nonstructural components. Additionally, the peak floor acceleration provides a basis for estimating damage to acceleration-sensitive moment-resisting components. The proposed procedure is aimed at situations in which economic losses are produced over a wide range of ground motion intensities.

Parameters of the probability distribution of structural response conditioned on ground motion intensity are computed from a relatively small number of deterministic response history structural analyses at three ground motion intensity levels. The proposed procedure explicitly takes into account the variation of central tendency and dispersion with changes in the loading intensity by using efficient curve-fitting procedures. The results are then combined with probabilistic estimates of ground motion intensity, obtained with a conventional probabilistic seismic hazard analysis, in order to estimate the annual probabilities of exceedance of the structural response parameters. The proposed procedure is evaluated when applied to an existing seven-story reinforced concrete building. The results are compared to those obtained with the SAC simplified procedure for estimating building response. The effects of various simplifying assumptions made in the SAC procedure are evaluated and discussed. It is concluded that the proposed procedure provides more accurate results with only a minimum additional computational effort.

ACKNOWLEDGMENT

This work was supported by the Pacific Earthquake Engineering Research Center through the Earthquake Engineering Research Centers Program of the National Science Foundation under award number EEC-9701568.

CONTENTS

LIST OF FIGURES

LIST OF TABLES

1 Introduction

The primary objective of performance-based earthquake engineering (PBEE) is to design facilities with predictable levels of performance. Levels of performance of a facility can be expressed qualitatively or quantitatively. Qualitative levels of performance are the current state of practice, FEMA 356, and are related to the structural characteristics of the facility based on engineering judgments. Quantitative levels of performance, however, allow for rigorously relating the performance levels of a facility to the structural characteristics of the facility.

Economic losses in a facility due to earthquakes represent a qualitative measure of seismic performance. Furthermore, it can be expressed as a continuum and can be related to the structural characteristics of the facility through a probabilistic framework. Economic losses in a facility can be categorized as direct and indirect losses. Direct losses are those associated with repair or replacement costs of building components, whereas indirect losses are those resulting from the temporary loss of function (downtime) of the facility.

In order to be able to predict the economic loss resulting from earthquake ground motions in a building or any other structure, it is first necessary to predict the response of the structure when subjected to earthquake ground motions of different levels of intensity. A probabilistic seismic hazard analysis (PSHA) is a rational procedure, which permits the estimation of the annual probability of exceedance of spectral ordinates at a given site by taking into account the location and seismicity of all possible seismic sources that can affect the site. A probabilistic seismic structural response analysis (PSSRA) extends a PSHA to the estimation of the annual probability of exceedance of the engineering demand parameter (*EDP*). One possible approach in PSSRA is to use the results of nonlinear response history analyses of the structure when subjected to acceleration time histories scaled to various levels of intensity.

Applying a suite of earthquake ground motion time histories scaled to various levels of intensity to evaluate the safety of structures subjected to earthquakes was first conceptually proposed by Bertero [1977]. Since then, many investigators have implemented this concept in various forms to estimate the response of various structures in seismic regions. For example,

Bazzurro and Cornell [1994] used the results of response history analyses to calculate the annual probability of offshore platform response exceeding specific performance levels. Miranda and his collaborators [1997, 2000] used a suite of earthquake ground motion time histories scaled to increasing levels of intensity to investigate the strength reduction factors of multi-degree-of-freedom (MDOF) structures required to adequately control maximum story displacement ductility demands under earthquake excitations. In their study, an iteration of the ground motion scaling factor was carried out until the maximum story displacement ductility demand in various buildings was, within a tolerance, equal to various target displacement ductility ratios considered as maximum tolerable.

Luco and Cornell [1998, 2000] developed a methodology that uses the results of nonlinear response history analyses to assess the probability of exceedance of maximum interstory drift ratios (*IDRs*) for evaluating the effects of fragile failure of moment-resisting connections in steel buildings. In particular, they proposed a simplified procedure to estimate the annual probability of exceedance of interstory drift ratios using an idealized seismic hazard curve. Mehanny and Deierlein [2000] also used the results of response history analyses applying accelerograms scaled to various levels of intensity to evaluate the seismic behavior of composite frames. Yun et al. [2001] used a similar approach to evaluate the performance of steel moment-resisting frame buildings as part of the SAC project.

More recently, the use of response history analyses applying accelerograms scaled at various levels of intensity to investigate the response of structures at various levels of ground motion intensity has been referred to as “dynamic pushover analysis” [Luco and Cornell 1998] or “incremental dynamic analysis” [Vamvatsikos and Cornell 2001]. This latter reference provides an overview of different possible variations and terminology associated with this type of analysis.

Presented in this report is a detailed study on PSSRA as a main step in building loss evaluation. In chapter 2 of this report, a loss estimation methodology is presented to estimate the building loss caused by earthquakes, in particular how PSSRA fits into the loss estimation methodology.

In chapter 3, the properties of a seven-story building, which is used as a case study for the implementation of PSSRA are presented. Different modeling assumptions that can be used in modeling the case study building are discussed. Also shown in this chapter is a detailed description of the ground motion time histories used in PSSRA.

A proposed procedure for the PSSRA implementation is presented in chapter 4. First, we describe the formulation to evaluate the probability of exceedance of the *EDP*. In the next step, we present the closed-form solution to evaluate the probability of exceedance of the *EDP* [Kennedy and Short 1994, Cornell 1996]. The simplifying assumptions upon which the closed-form solution is developed are then evaluated. Based on this evaluation, a generic approach is proposed to estimate the probability of exceedance of different types of *EDPs* at a wide range of levels of deformation. The approach explicitly takes into account the variation of central tendency and dispersion of the *EDP* with the changes in the level of ground motion intensity. Further, a procedure is proposed that provide better estimates of the probability distribution of *EDPs* at a given level of intensity. The results from the implementation of the proposed procedure to a seven-story reinforced concrete building, described in chapter 3, are then compared to the results of a more accurate procedure, to determine the efficiency of the proposed approach.

Although the proposed procedure is quite generic and can be applied to any type of *EDP*, here only maximum interstory drifts at all stories and maximum floor accelerations at all levels are examined in more detail. Both of these parameters are well correlated with structural as well as with moment-resisting damage, so they provide an excellent basis to estimate the performance of structures during earthquakes.

2 Loss Estimation Formulation

The aim of PEER's loss estimation efforts is to describe seismic performance quantitatively by continuous variables rather than discrete and sometimes subjective performance levels. The building-specific loss estimation methodology described in this report provides such continuous and quantitative measure of seismic performance in terms of economic losses in a specific building. In particular, the ultimate goal is to compute the mean annual probability of exceedance of different levels of dollar losses. This information will allow decision makers to respond to questions such as What is the probability of facing an economic loss higher than $1.0 million in my structure? In this chapter, however, we concentrate on summarizing our efforts aimed at the estimation of the expected annual loss in the building, $E[L_{Bldg}]$, that corresponds to the average loss that owners have every year in their building structure. Consequently, the decision variable, *DV*, in this investigation is the expected annual loss in the building, i.e., $DV=E[L_{Bldg}]$.

The *PEER* framework equation is given by [Cornell and Krawinkler 2000]:

$$\lambda(DV) = \iint G(DV \mid DM)\, dG(DM \mid IM)\, d\lambda(IM) \tag{2.1}$$

where $G(DV|DM)$ is the probability that the decision variable exceeds specified values given (i.e., conditional on knowing) that the engineering damage measures (e.g., the maximum interstory drift, and/or the vector of cumulative hysteretic energies in all elements) are equal to particular values. Further, $G(DM|IM)$ is the probability that the damage measure(s) exceed these values given that the intensity measure(s) (such as spectral acceleration at the fundamental mode frequency, and/or spectral shape parameters and/or duration) equal particular values. Finally, $\lambda(IM)$ is the mean annual frequency of the intensity measure(s) which for small values is equal to the annual probability of exceedance of the intensity measure(s).

More recently, Krawinkler (2002) modified the above equation to more adequately distinguish between structural response parameters such as interstory drift ratio, absolute floor acceleration, and cumulative hysteretic energy from different damage states in structural and

nonstructural components. The first are referred to as "engineering demand parameters" (*EDPs*), while the damage states are referred to as "damage measures" (*DMs*). The modified framework equation is given by

$$\lambda(DV) = \iiint G(DV \mid DM)\,dG(DM \mid EDP)\,dG(EDP \mid IM)\,d\lambda(IM) \tag{2.2}$$

Equation (2.2) assumes that all four variables (*IM, EDP, DM, and DV*) are continuous random variables. However, economic losses in individual components are associated with repair actions, which may be discretely triggered at certain levels of damage. For example, the replacement of glass in a window is triggered when the glass is cracked or broken, so in these cases the damage measures become discrete and the above equation needs to be modified, as will be shown below.

In order to compute the mean annual frequency of exceedance in the building, it is first necessary to compute the losses in individual components. The annual probability of exceeding a loss level l in the j^{th} component (either a structural or moment-resisting component) considering discrete damage states is given by

$$P[L_j > l] = \sum_{i=1}^{m} \int_0^\infty \int_0^\infty P[L_l > l \mid DM = dm_i]\, P(DM = dm_i \mid EDP_j = edp) \left| dP(EDP_j > edp \mid IM = im) \right| \left| \frac{d\nu(IM)}{dIM} \right| dIM \tag{2.3}$$

where m is the number of damage states in jth component, $P[L_j > l \mid DM = dm_i]$ is the annual probability of exceedance of a loss l in the jth component conditioned on knowing that the component is in the ith damage state, $P(DM = dm_i \mid EDP_j = edp)$ is the probability that the jth component will be in damage state i given that the component has been subjected to an *EDP* equal to *edp*, $P(EDP_j > edp \mid IM = im)$ is the probability that the *EDP* affecting component j will exceed a certain value *edp* given that the ground motion intensity measure *IM* is equal to *im*, and finally $\left| \frac{d\nu(IM)}{dIM} \right|$ is the slope of the seismic hazard curve corresponding to the intensity measure *IM*.

In Equation (2.3) the probability that the jth component will be in damage state i given that component has been subjected to an *EDP* equal to *edp* is computed as

$$P(DM_j = dm_i \mid EDP_j = edp) = P(DM_j > dm_i \mid EDP_j = edp) - P(DM_j > dm_{i+1} \mid EDP_j = edp) \tag{2.4}$$

where $P(DM_j > dm_i \mid EDP_j = edp)$ is the probability of exceeding damage state i in the j^{th} component given that it has been subjected to an EDP equal to edp, $P(DM_j > dm_{i+1} \mid EDP_j = edp)$ is the probability of exceeding damage state i+1 in the j^{th} component given that it has been subjected to an EDP equal to edp. Functions $P(DM_j > dm_i \mid EDP_j = edp)$ and $P(DM_j > dm_{i+1} \mid EDP_j = edp)$ correspond to the ith and ith+1 fragility functions of a j^{th} component as a function of EDP, which describe the vulnerability or damageability of the j^{th} component with increasing levels of EDP.

The expected annual loss in the j^{th} component is obtained by replacing $P[L_j > l \mid DM = dm_i]$ in Equation (2.3) by the expected value of the loss in the j^{th} component given that it is in damage state i, $E[L_j \mid DM = dm_i]$, as follows:

$$E[L_j] = \sum_{i=1}^{m} \int_0^{\infty} \int_0^{\infty} E[L_j \mid DM = dm_i]\, P(DM = dm_i \mid EDP_j = edp) \left| dP(EDP_j > edp \mid IM = im) \right| \left| \frac{d\nu(IM)}{dIM} \right| dIM \quad (2.5)$$

The expected annual loss for the whole building resulting from direct physical damage is then computed as the sum of the expected losses in each individual component in the building, that is

$$E[L_{Bldg.}] = E[L_{j=1}] + E[L_{j=2}] + E[L_{j=3}] + \ldots + E[L_{j=n}] = \sum_{j=1}^{n} E[L_j] \quad (2.6)$$

where n is the total number of components in the building.

Although the summation and integrals in Equation (2.5) can be solved in any order, certain sequences provide intermediate results that also provide valuable information to the structural engineer, owner(s) and the interested parties of the seismic performance of the building.

For example, the expected value of the loss in jth component given that it has been subjected to an engineering demand parameter can be computed as

$$E[L_j \mid EDP_j = edp] = \sum_{i=1}^{m} E[L_j \mid DM = dm_i]\, P(DM = dm_i \mid EDP_j = edp) \quad (2.7)$$

where $P(DM = dm_i \mid EDP_j = edp)$ is given by Equation (2.4). Then the variation (increase) of dollar loss in the jth component with changes (increase) in EDP can then be obtained by plotting

EDPj versus $E[L_j \mid EDP_j = edp]$. Similarly, the variation of dollar loss from drift-sensitive structural and nonstructural components in the *k*th floor of the building can be obtained by plotting EDP_k versus $\sum_{j=1}^{p} E[L_j \mid EDP_j = edp]$ where *p* is the number of drift-sensitive components in the *k*th floor of the building.

Similarly, the expected value of the dollar loss in the *j*th component, given that the building has been subjected to a ground motion with intensity *im* can be computed as

$$E[L_j \mid IM = im] = \int_0^\infty E[L_j \mid EDP_j = edp] \left| dP(EDP_j > edp \mid IM = im) \right| \tag{2.8}$$

The expected value of the dollar loss in the building as a function of the level of ground motion intensity is hence computed as

$$E[L_{Bldg} \mid IM = im] = \sum_{j=1}^{n} E[L_j \mid IM = im] \tag{2.9}$$

A plot of *IM* versus $E[L_{Bldg} \mid IM = im]$ provides information on how the expected value of the loss (i.e., the average loss in the building) increases when the ground motion intensity increases.

Finally the expected annual loss in the building can be computed as

$$E[L_{Bldg}] = \int_0^\infty E[L_{Bldg} \mid IM = im] \left| d\nu(IM) \right| \tag{2.10}$$

where $d\nu(IM)$ can be written as

$$\left| d\nu(IM) \right| = \left| \frac{d\nu(IM)}{dIM} \right| dIM \tag{2.11}$$

Substituting (2.11) in (2.10)

$$E[L_{Bldg}] = \int_0^\infty E[L_{Bldg} \mid IM = im] \left| \frac{d\nu(IM)}{dIM} \right| dIM \tag{2.12}$$

This report concentrates on the evaluation of $P(EDP_j > edp \mid IM = im)$ for individual components.

3 Building Modeling and Loading Assumptions

3.1 GENERAL CHARACTERISTICS

In this study an existing seven-story reinforced concrete structure has been selected for the implementation of the PSSRA methodology. The building is located in Van Nuys, California, approximately in the middle of San Fernando Valley in the northern section of the greater Los Angeles metropolitan area. The building was designed in 1965 and built in 1966. The approximate construction cost of the building was $1.3 million in 1966 dollars [Blume et al. 1973]. Figure 3.1 shows the south elevation of the building. Figure 3.2 presents the north elevation and plan of the building.

Fig. 3.1 Elevation view of the building considered in this study [after Naeim 1997].

The building is currently instrumented by the California Strong Motion Instrumentation Program (CSMIP) run by the California Division of Mines and Geology of the State of California. A list of ground motions recorded in the building is presented in Table 3.1. Of these earthquakes two of them, the San Fernando earthquake and Northridge earthquake caused significant damage in the building. The 1971 San Fernando earthquake, induced a damage corresponding to 11% of the total building cost. The structural damage occurred in the building due to this earthquake was 0.2% of the building total cost and the rest of the damage occurred in moment-resisting components. The average repair cost for the building was $2.30 per square foot in 1966 dollars.

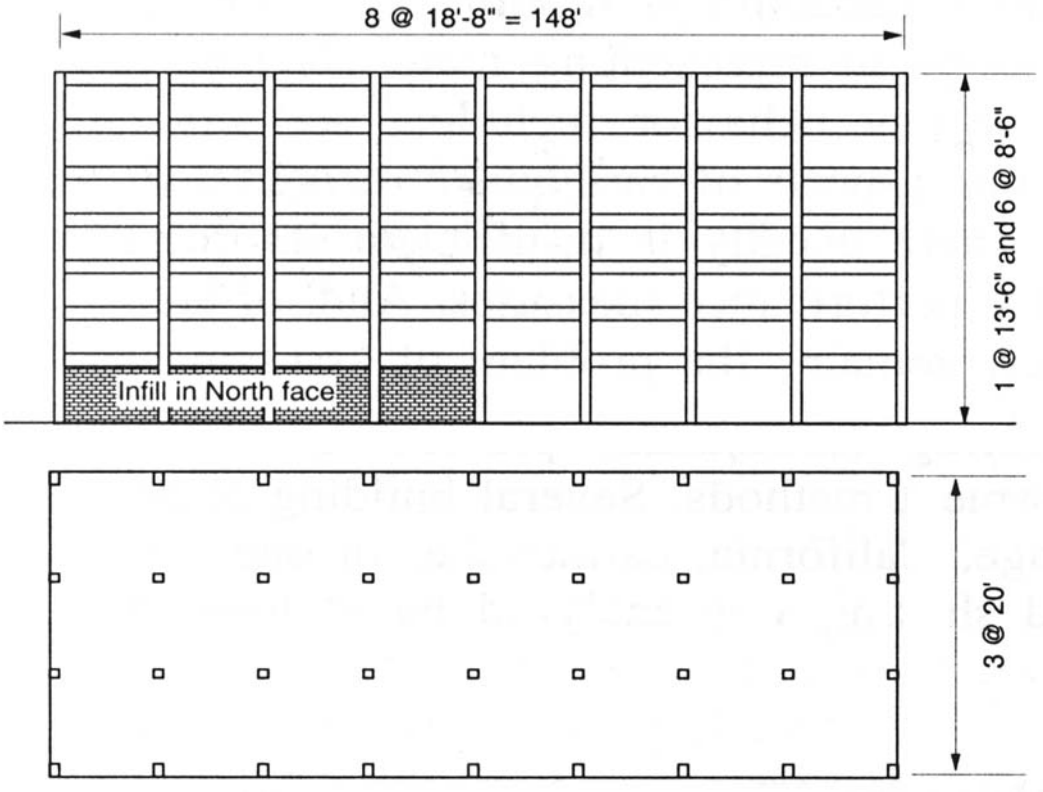

Fig. 3.2 Schematic view of the north elevation of the building and the plan of the building [after Browning et al. 2000].

The 1994 Northridge earthquake caused severe structural and moment-resisting damage in the building. The most severe structural damage in the building was the shear failure of four

exterior columns in the fourth story in the south face of the building. Figure 3.3 presents photographs of these shear failures in some of the exterior columns of the building.

Table 3.1 Earthquake ground motions recorded in the building

Earthquake	Event Time	Magnitude
San Fernando	9-Feb-71	6.7
Whittier	1-Oct-87	6.1
Landers	28-Jun-92	7.6
Big Bear	28-Jun-92	6.6
Northridge	17-Jan-94	6.7

Fig. 3.3 Examples of structural damage in the building due to 1994 Northridge earthquake; shear failure of columns in the south face at fifth story. [After Naeim 1997].

3.2 STRUCTURAL PROPERTIES OF THE BUILDING

The structural system of the building is composed of perimeter moment-resisting frames and interior gravity-resisting frames (flat slabs and columns). Table 3.2 presents the dimensions of the structural elements of the Van Nuys building. It can be seen from the table that the slab thickness decreases in the upper stories of the building. At the second floor the slab has a thickness of 25 cm (10 in.), whereas in the third to seventh floors the slab thickness is 21.25 cm (8.5 in.). The slab thickness at the roof level is 20 cm (8 in.). The exterior columns are rectangular, 50 x 35 cm (20 x 14 in.) with constant dimensions throughout the height of the building. The dimensions of the spandrel beams are almost the same for the longitudinal and transverse directions. The beam dimensions decrease, however, in the upper stories. At the second floor the longitudinal beams are 75 x 40 cm (30 x 16 in.) and the transverse ones are 75 x 35 cm (30 x 14 in.). For the third to seventh floors the height of the spandrel beams decrease from 75 cm (30 in.) to 56.25 cm (22.5 in.). The columns weak axis is perpendicular to the longitudinal direction. The interior columns have a square section of 50 x 50 cm (20 x 20 in.) at the first story, which decreases to 45 x 45cm (18 x 18 in.) in the upper stories.

Table 3.2 Dimensions of structural members of the building used in this study

Location in the structure	Slab Thickness	Longitudinal Spandrel Beams	Transverse Spandrel Beams	Exterior Columns Sections [1]	Interior Columns Sections
	cm	cm x cm	cm x cm	cm x cm	cm x cm
Ground Floor	10	-	-		
				50 x 35	50 x 50
2nd Floor	25	75 x 40	75 x 35		
				50 x 35	45 x 45
Typical Floor	21.25	56.25 x 40	56.25 x 35		
				50 x 35	45 x 45
Roof (8th Floor)	20	55 x 40	55 x 35		
[1] Exterior Columns Weak Axis is in Longitudinal (East-West) Direction					

Table 3.3 presents the material properties used in different structural elements of the building. The concrete nominal compressive strength ranges from 20.7 MPa (3000 psi) to 34.4 MPa (5000 psi), while the nominal yielding stress of the reinforcing steel for beams and slabs is 276 MPa (40 ksi) and for columns is 414 MPa (60 ksi).

3.3 BUILDING LOADING ASSUMPTIONS

The structure was analyzed using response history analyses applying a suite of 79 earthquake ground motions recorded in various earthquakes in California. All ground motions were recorded on free-field sites that can be classified as site class D according to recent NEHRP seismic provisions [BSSC 1997]). Ground motions have been carefully selected [Medina 2001] from the Pacific Earthquake Engineering Research (PEER) Center strong motion database where all ground motions have been processed with the same procedure. The earthquake magnitudes for the selected records ranges from 5.8 to 6.9, with the closest distances to rupture varying from 13 km to 60 km. Figure 3.4 shows the distribution of magnitude and distance to the source for the earthquake ground motions used in this study. Table 3.3 presents the detailed information for each of the earthquake time histories used in this study.

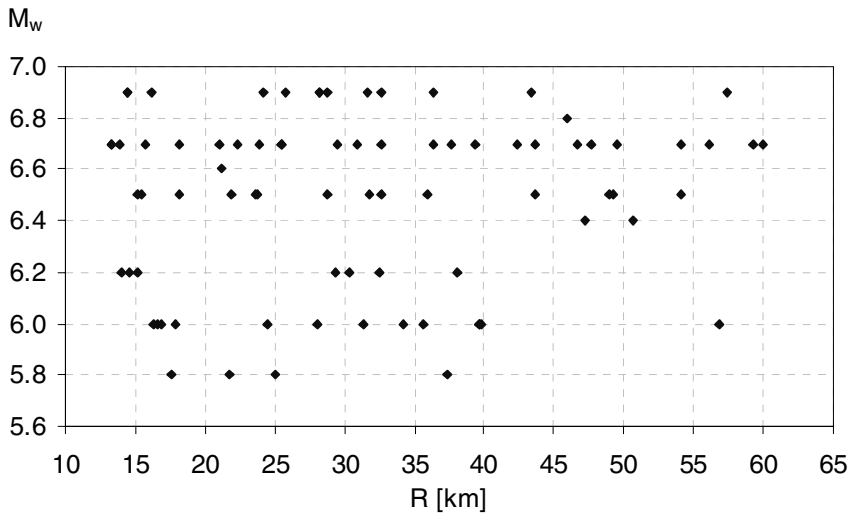

Fig. 3.4 Magnitudes and the closest distance to the rupture of ground motions used in this study

Table 3.3 Detailed characteristics of the earthquake ground motions used in this study

Record ID	Event	Year	Magnitude	Station	R (km)	NEHRP Soil	Mechanism	fHP (Hz)	fLP (Hz)	PGA (g)	PGV (cm/s)	PGD (cm)	Rec. Length (s)
IV79cal	Imperial Valley	1979	6.5	Calipatria Fire Station	23.8	D	strike-slip	0.10	40.0	0.078	13.3	6.2	39.5
IV79chi	Imperial Valley	1979	6.5	Chihuahua	28.7	D	strike-slip	0.05		0.270	24.9	9.1	40.0
IV79e01	Imperial Valley	1979	6.5	El Centro Array #1	15.5	D	strike-slip	0.10	40.0	0.139	16.0	10.0	39.5
IV79e12	Imperial Valley	1979	6.5	El Centro Array #12	18.2	D	strike-slip	0.10	40.0	0.116	21.8	12.1	39.0
IV79e13	Imperial Valley	1979	6.5	El Centro Array #13	21.9	D	strike-slip	0.20	40.0	0.139	13.0	5.8	39.5
IV79qkp	Imperial Valley	1979	6.5	Cucapah	23.6	D	strike-slip	0.05		0.309	36.3	10.4	40.0
IV79wsm	Imperial Valley	1979	6.5	Westmoreland Fire Station	15.1	D	strike-slip	0.10	40.0	0.110	21.9	10.0	40.0
LV80kod	Livermore	1980	5.8	San Ramon Fire Station	21.7	D	strike-slip	0.20	15.0	0.040	4.0	1.2	21.0
LV80srm	Livermore	1980	5.8	San Ramon - Eastman Kodak	17.6	D	strike-slip	0.20	20.0	0.076	6.1	1.7	40.0
MH84g02	Morgan Hill	1984	6.2	Gilroy Array #2	15.1	D	strike-slip	0.20	31.0	0.162	5.1	1.4	30.0
MH84g03	Morgan Hill	1984	6.2	Gilroy Array #3	14.6	D	strike-slip	0.10	37.0	0.194	11.2	2.4	40.0
MH84gmr	Morgan Hill	1984	6.2	Gilroy Array #7	14.0	D	strike-slip	0.10	30.0	0.113	6.0	1.8	30.0
PM73phn	Point Mugu	1973	5.8	Port Hueneme	25.0	D	reverse-slip	0.20	25.0	0.112	14.8	2.6	23.2
PS86psa	N. Palm Springs	1986	6.0	Palm Springs Airport	16.6	D	strike-slip	0.20	60.0	0.187	12.2	2.1	30.0
WN87cas	Whittier Narrows	1987	6.0	Compton - Castlegate St.	16.9	D	reverse	0.09	25.0	0.332	27.1	5.0	31.2
WN87cat	Whittier Narrows	1987	6.0	Carson - Catskill Ave.	28.1	D	reverse	0.18	25.0	0.042	3.8	0.8	32.9
WN87flo	Whittier Narrows	1987	6.0	Brea - S Flower Ave.	17.9	D	reverse	0.16	25.0	0.115	7.1	1.2	27.6
WN87w70	Whittier Narrows	1987	6.0	LA - W 70th St.	16.3	D	reverse	0.20	25.0	0.151	8.7	1.5	31.9
WN87wat	Whittier Narrows	1987	6.0	Carson - Water St.	24.5	D	reverse	0.20	25.0	0.104	9.0	1.9	29.7
LP89agw	Loma Prieta	1989	6.9	Agnews State Hospital	28.2	D	reverse-oblique	0.20	30.0	0.172	26.0	12.6	40.0
LP89cap	Loma Prieta	1989	6.9	Capitola	14.5	D	reverse-oblique	0.20	40.0	0.443	29.3	5.5	40.0
LP89g03	Loma Prieta	1989	6.9	Gilroy Array #3	14.4	D	reverse-oblique	0.10	40.0	0.367	44.7	19.3	39.9
LP89g04	Loma Prieta	1989	6.9	Gilroy Array #4	16.1	D	reverse-oblique	0.20	30.0	0.212	37.9	10.1	40.0
LP89gmr	Loma Prieta	1989	6.9	Gilroy Array #7	24.2	D	reverse-oblique	0.20	40.0	0.226	16.4	2.5	40.0
LP89hch	Loma Prieta	1989	6.9	Hollister City Hall	28.2	D	reverse-oblique	0.10	29.0	0.247	38.5	17.8	39.1
LP89hda	Loma Prieta	1989	6.9	Hollister Differential Array	25.8	D	reverse-oblique	0.10	33.0	0.279	35.6	13.1	39.6
LP89svl	Loma Prieta	1989	6.9	Sunnyvale - Colton Ave.	28.8	D	reverse-oblique	0.10	40.0	0.207	37.3	19.1	39.3
NR94cnp	Northridge	1994	6.7	Canoga Park - Topanga Can.	15.8	D	reverse-slip	0.05	30.0	0.420	60.8	20.2	25.0
NR94far	Northridge	1994	6.7	LA - N Faring Rd.	23.9	D	reverse-slip	0.13	30.0	0.273	15.8	3.3	30.0
NR94fle	Northridge	1994	6.7	LA - Fletcher Dr.	29.5	D	reverse-slip	0.15	30.0	0.240	26.2	3.6	30.0
NR94glp	Northridge	1994	6.7	Glendale - Las Palmas	25.4	D	reverse-slip	0.10	30.0	0.206	7.4	1.8	30.0
NR94hol	Northridge	1994	6.7	LA - Hollywood Stor FF	25.5	D	reverse-slip	0.20	23.0	0.231	18.3	4.8	40.0
NR94nya	Northridge	1994	6.7	La Crescenta-New York	22.3	D	reverse-slip	0.10	0.3	0.159	11.3	3.0	30.0
NR94stc	Northridge	1994	6.7	Northridge - 17645 Saticoy St.	13.3	D	reverse-slip	0.10	30.0	0.368	28.9	8.4	30.0
SF71pel	San Fernando	1971	6.6	LA - Hollywood Stor Lot	21.2	D	reverse-slip	0.20	35.0	0.174	14.9	6.3	28.0
SH87bra	Superstition Hills	1987	6.7	Brawley	18.2	D	strike-slip	0.10	23.0	0.156	13.9	5.4	22.1
SH87icc	Superstition Hills	1987	6.7	El Centro Imp. Co. Cent	13.9	D	strike-slip	0.10	40.0	0.358	46.4	17.5	40.0
SH87pls	Superstition Hills	1987	6.7	Plaster City	21.0	D	strike-slip	0.20	18.0	0.186	20.6	5.4	22.2
SH87wsm	Superstition Hills	1987	6.7	Westmoreland Fire Station	13.3	D	strike-slip	0.10	35.0	0.172	23.5	13.0	40.0

Table 3.3—*Continued.* Detailed characteristics of the earthquake ground motions used in this study

Record ID	Event	Year	Magnitude	Station	R (km)	NEHRP Soil	Mechanism	fHP (Hz)	fLP (Hz)	PGA (g)	PGV (cm/s)	PGD (cm)	Rec. Length (s)
BM68elc	Borrego Mountain	1968	6.8	El Centro Array #9	46.0	D	strike-slip	0.20	12.8	0.057	13.2	10.0	40.0
LP89a2e	Loma Prieta	1989	6.9	APEEL 2E Hayward Muir Sch.	57.4	D	reverse-oblique	0.20	30.0	0.171	13.7	3.9	40.0
LP89fms	Loma Prieta	1989	6.9	Fremont - Emerson Court	43.4	D	reverse-oblique	0.10	32.0	0.141	12.9	8.4	39.7
LP89hvr	Loma Prieta	1989	6.9	Halls Valley	31.6	D	reverse-oblique	0.20	22.0	0.134	15.4	3.3	40.0
LP89sjw	Loma Prieta	1989	6.9	Salinas - John & Work	32.6	D	reverse-oblique	0.10	28.0	0.112	15.7	7.9	40.0
LP89slc	Loma Prieta	1989	6.9	Palo Alto - SLAC Lab.	36.3	D	reverse-oblique	0.20	33.0	0.194	37.5	10.0	39.6
NR94bad	Northridge	1994	6.7	Covina - W. Badillo	56.1	D	reverse-slip	0.20	30.0	0.100	5.8	1.2	35.0
NR94cas	Northridge	1994	6.7	Compton - Castlegate St.	49.6	D	reverse-slip	0.20	30.0	0.136	7.1	2.2	39.8
NR94cen	Northridge	1994	6.7	LA - Centinela St.	30.9	D	reverse-slip	0.20	30.0	0.322	22.9	5.5	30.0
NR94del	Northridge	1994	6.7	Lakewood - Del Amo Blvd.	59.3	D	reverse-slip	0.13	30.0	0.137	11.2	2.0	35.4
NR94dwn	Northridge	1994	6.7	Downey - Co. Maint. Bldg.	47.6	D	reverse-slip	0.20	23.0	0.158	13.8	2.3	40.0
NR94jab	Northridge	1994	6.7	Bell Gardens - Jaboneria	46.6	D	reverse-slip	0.13	30.0	0.068	7.6	2.5	35.0
NR94lh1	Northridge	1994	6.7	Lake Hughes #1	36.3	D	reverse-slip	0.12	23.0	0.087	9.4	3.7	32.0
NR94loa	Northridge	1994	6.7	Lawndale - Osage Ave.	42.4	D	reverse-slip	0.13	30.0	0.152	8.0	2.6	40.0
NR94lv2	Northridge	1994	6.7	Leona Valley #2	37.7	D	reverse-slip	0.20	23.0	0.063	7.2	1.6	32.0
NR94php	Northridge	1994	6.7	Palmdale - Hwy 14 & Palmdale	43.6	D	reverse-slip	0.20	46.0	0.067	16.9	8.0	60.0
NR94pic	Northridge	1994	6.7	LA - Pico & Sentous	32.7	D	reverse-slip	0.20	46.0	0.186	14.3	2.4	40.0
NR94sor	Northridge	1994	6.7	West Covina - S. Orange Ave.	54.1	D	reverse-slip	0.20	30.0	0.063	5.9	1.3	36.5
NR94sse	Northridge	1994	6.7	Terminal Island - S. Seaside	60.0	D	reverse-slip	0.13	30.0	0.194	12.1	2.3	35.0
NR94ver	Northridge	1994	6.7	LA - E Vernon Ave.	39.3	D	reverse-slip	0.10	30.0	0.153	10.1	1.8	30.0
BO42elc	Borrego	1942	6.5	El Centro Array #9	49.0	D		0.10	15.0	0.068	3.9	1.4	40.0
CO83c05	Coalinga	1983	6.4	Parkfield - Cholame 5W	47.3	D	reverse-oblique	0.20	22.0	0.131	10.0	1.3	40.0
CO83c08	Coalinga	1983	6.4	Parkfield - Cholame 8W	50.7	D	reverse-oblique	0.20	23.0	0.098	8.6	1.5	32.0
IV79cc4	Imperial Valley	1979	6.5	Coachella Canal #4	49.3	D	strike-slip	0.20	40.0	0.128	15.6	3.0	28.5
IV79cmp	Imperial Valley	1979	6.5	Compuertas	32.6	D	strike-slip	0.20		0.186	13.9	2.9	36.0
IV79dlt	Imperial Valley	1979	6.5	Delta	43.6	D	strike-slip	0.05		0.238	26.0	12.1	99.9
IV79nil	Imperial Valley	1979	6.5	Niland Fire Station	35.9	D	strike-slip	0.10	30.0	0.109	11.9	6.9	40.0
IV79pls	Imperial Valley	1979	6.5	Plaster City	31.7	D	strike-slip	0.10	40.0	0.057	5.4	1.9	18.7
IV79vct	Imperial Valley	1979	6.5	Victoria	54.1	D	strike-slip	0.20		0.167	8.3	1.1	40.0
LV80stp	Livermore	1980	5.8	Tracy - Sewage Treatment Plant	37.3	D	strike-slip	0.08	15.0	0.073	7.6	1.8	33.0
MH84cap	Morgan Hill	1984	6.2	Capitola	38.1	D	strike-slip	0.20	30.0	0.099	4.9	0.6	36.0
MH84hch	Morgan Hill	1984	6.2	Hollister City Hall	32.5	D	strike-slip	0.20	19.0	0.071	7.4	1.6	28.3
MH84sjb	Morgan Hill	1984	6.2	San Juan Bautista	30.3	C	strike-slip	0.10	21.0	0.036	4.4	1.5	28.0
PS86h06	N. Palm Springs	1986	6.0	San Jacinto Valley Cemetery	39.6	D	strike-slip	0.20	31.0	0.063	4.4	1.2	40.0
PS86ino	N. Palm Springs	1986	6.0	Indio	39.6	D	strike-slip	0.10	35.0	0.064	6.6	2.2	30.0
WN87bir	Whittier Narrows	1987	6.0	Downey - Birchdale	56.8	D	reverse	0.15	25.0	0.299	37.8	5.0	28.6
WN87cts	Whittier Narrows	1987	6.0	LA - Century City CC South	31.3	D	reverse	0.20	25.0	0.051	3.5	0.6	40.0
WN87har	Whittier Narrows	1987	6.0	LB - Harbor Admin FF	34.2	D	reverse	0.25	25.0	0.071	7.3	0.9	40.0
WN87sse	Whittier Narrows	1987	6.0	Terminal Island - S. Seaside	35.7	D	reverse	0.20	25.0	0.042	3.9	1.0	22.9
WN87stc	Whittier Narrows	1987	6.0	Northridge - Saticoy St.	39.8	D	reverse	0.20	25.0	0.118	5.1	0.8	40.0

4 Probabilistic Seismic Structural Response Analysis for Loss Estimation

4.1 FORMULATION

The conditional probability of occurrence of an event E_1, knowing that event E_2 has occurred, is defined as

$$P(E_1 \mid E_2) = \frac{P(E_1 \cap E_2)}{P(E_2)} \tag{4.1}$$

where $P(E_1 \cap E_2)$ is the probability of the combined occurrence of events E_1 and E_2; and $P(E_2)$ is the probability of occurrence of event E_2. Solving for $P(E_1 \cap E_2)$ in (1) we have that the probability of the combined occurrence of events E_1 and E_2 is given by

$$P(E_1 \cap E_2) = P(E_1 \mid E_2)\ P(E_2) \tag{4.2}$$

By using Equation (4.2) and the total probability theorem, for n mutually exclusive and collectively exhaustive events E_i, the probability of occurrence of an event A can be computed as

$$P(A) = \sum_{i=1}^{n} P(A \mid E_i)\ P(E_i) \tag{4.3}$$

in which $P(A|E_i)$ is the probability of occurrence of event A, conditioned on the occurrence of event E_i, and $P(E_i)$ is the probability of occurrence of event E_i.

Modifying the total probability theorem for continuous random variables, we have

$$P(A) = \int_{-\infty}^{\infty} P(A \mid E)\, \mathrm{d}P(E) \tag{4.4}$$

In *PBEE* Equation (4.4) can be used to estimate the annual probability of occurrence of any *EDP* against a particular value *edp* as follows:

$$P(EDP < edp) = \int_0^{\infty} P(EDP < edp \mid IM = im)\, dP(IM) \tag{4.5}$$

where *P(IM)* is the annual probability of occurrence of the ground motion intensity *IM*; *P(EDP < edp | IM = im)* is the probability that the engineering demand parameter is smaller than a certain level *edp* given that the ground motion has an intensity of *im*.

Similarly, the annual probability of an engineering demand parameter exceeding level *edp* is given by

$$P(EDP > edp) = \int_0^{\infty} \left[1 - P(EDP < edp \mid IM = im)\right] \left|\frac{d\nu(IM)}{dIM}\right| dIM \tag{4.6}$$

In Equation (4.6) the first factor in the integrand corresponds to the estimation of the structural response for a given ground motion intensity which can be obtained with a probabilistic structural analysis, while the second factor represents the slope of the seismic hazard curve evaluated at an intensity *im*, which can be computed using a conventional PSHA. Thus, this equation permits the integration of the results from structural engineers in the first factor with results from seismologists in the second factor.

For Equations (4.5) and (4.6) to be valid, the conditional probability of occurrence of *EDP* should depend only on the ground motion intensity measure *IM* and not on the factors affecting the intensity measure itself. For example, if the intensity measure is a linear elastic spectral ordinate that depends primarily on the earthquake magnitude and the distance to the source, then, the conditional probability of the occurrence of *EDP* should not depend on the earthquake magnitude nor on the distance to the source.

The dependency of different types of structural response on earthquake magnitude and distance has been investigated by different researchers. Sewell [1989] studied the influence of earthquake magnitude and distance on an inelastic effective factor, representing the level of damage in the structure. Miranda [1993, 1991] studied the effect of magnitude and distance on the strength reduction factors and inelastic displacement ratios, and systems undergoing different levels of displacement ductility [Miranda 2000]. Miranda and Aslani [2003] studied the effect of magnitude and distance on the conditional probability of engineering demand parameters of MDOF systems conditioned to the ground motion intensity.

Equations equal or similar to (4.5) and (4.6) have been used extensively in earthquake engineering. For example, Esteva [1980] used this approach to compute the probability of

occurrence of earthquake losses. Sewell [1989] used it to evaluate the probability of exceedance of nonlinear damage thresholds. Shome and Cornell [1999] used it for the estimation of the likelihood of exceeding a damage measure. Ordaz et al. [2000] used an equation similar to Equation (4.6) to compute losses due to earthquake in structures in Mexico City.

4.2 SIMPLIFIED APPROACH

It is possible to obtain a closed-form solution to Equation (4.6) [Kennedy and Short 1994, Cornell 1996]. The following simplifying assumptions are made to obtain a closed-form solution to Equation (4.6) for maximum interstory drift ratio (*IDR)* in multistory buildings:

1. The probability of occurrence of the maximum interstory drift ratio conditioned to the occurrence of a given spectral ordinate is assumed to be lognormally distributed as follows

$$P(IDR|\ S_a)=\Phi\left(\frac{\mathrm{Ln}(IDR)-\mu_{\mathrm{Ln}\ IDR|S_a}}{\sigma_{\mathrm{Ln}\ IDR\ |S_a}}\right) \tag{4.7}$$

   where Φ is the cumulative normal distribution function and $\mu_{\mathrm{Ln}\ IDR|Sa}$ is the mean of the natural log of the maximum interstory drift ratio, occurring at any story of the structure for a given spectral ordinate, and $\sigma_{\mathrm{Ln}\ IDR|Sa}$ is a measure of dispersion computed as the standard deviation of the natural log of the interstory drift ratio.

2. The seismic hazard curve of the pseudo-acceleration spectral ordinate, S_a, (i.e., the annual rate of exceedance of S_a) corresponding to the fundamental period of vibration of the structure is assumed to have an exponential functional form as follows:

$$\upsilon(S_a)=k_0(S_a)^{-k} \tag{4.8}$$

   where k_0 and k are constants. Cornell and Kennedy [1994], and Cornell [1996] proposed the use of this equation for obtaining the closed-form solution to Equation (4.6). Equation (4.8) implies that the seismic hazard curve is assumed to be linear when plotted in log-log paper. The evaluation of parameters k_0 and k is discussed in the next section.

3. The variation of the median of the maximum interstory drift ratio (or other engineering demand parameter) with changes in the linear elastic spectral ordinate at the fundamental period of the structure is assumed to have the following form:

$$\exp\left[\mu_{LnIDR|S_a}\right] = a(S_a)^b \tag{4.9}$$

where a and b are constants that control the slope and degree of nonlinearity, respectively. In particular, for b=1 the median of the interstory drift ratio is assumed to be linearly proportional to S_a.

4. The dispersion of the interstory drift is assumed constant with changes in the ground motion intensity (with changes in S_a). Two recommendations have been proposed for the evaluation of this dispersion parameter. Luco and Cornell [1997] used a global measure of dispersion corresponding to the dispersion computed over a range of spectral ordinates. In another study, Luco and Cornell [1998] state that a dispersion corresponding to any given intensity level of interest can be used. In both cases the dispersion parameter used in Equation (4.7) is assumed constant. In this study the dispersion at the intensity level associated with earthquakes with the probability of exceedance equal to 10% in 50 years has been used for evaluating the simplified closed-form procedure.

With the above simplifying assumptions, the annual rate of exceedance of the maximum interstory drift ratio can be computed [Luco and Cornell 1998, 2000; Kennedy and Short 1994] as

$$\nu(IDR) = k_0 \left[\left(\frac{IDR}{a}\right)^{\frac{1}{b}}\right]^{-k} \exp\left[\frac{1}{2}k^2\left(\frac{\sigma_{\ln IDR|Sa}}{b}\right)^2\right] \tag{4.10}$$

4.3 EVALUATION OF SIMPLIFYING ASSUMPTIONS

In order to evaluate the validity of the simplifying assumptions mentioned in the previous section, an investigation was done using the case study building described in chapter 3.

Based on the original structural drawings of the building, a model was developed for the longitudinal direction. The model consists of an exterior frame linked to an interior frame by axially rigid links, such that both types of frames undergo the same lateral displacement. Some of the most relevant modeling assumptions are

(a) Strength and stiffness of all members were based on moment-curvature relationships that considered the presence of gravity loads.

(b) Strength of reinforcing bars and concrete were increased 25% from their nominal values, respectively, to account for material overstrength.

(c) Half of the connection dimension was assumed rigid in beam-column connections, and the slab was considered to contribute to both strength and stiffness of the beams with an equivalent width of one twelfth of the span length.

(d) The equivalent slab width of interior slab-column connections was based on the recommendations by Hwang and Moehle [1993].

(e) The effect of gravity loads and the second-order deformations, P-Δ effects, was considered using a geometric stiffness formulation.

The model of the building with the above assumptions had a first period of vibration equal to 1.59 s [Miranda and Aslani 2001]. The structure was analyzed using response history analyses applying the suite of 79 earthquake ground motions presented in chapter 3.

For each ground motion the response of the structure was obtained at seven different intensity levels, by scaling the ground motions to have a linear elastic spectral displacement ordinate equal to 2.5, 10, 20, 30, 40, 50 and 60 cm (1, 4, 8, 12, 16, 20, and 24 in.). These spectral ordinates were computed for a system with a period of vibration equal to the fundamental period of vibration of the building and 5% damping ratio. Two types of *EDP*s were evaluated. The first type of *EDP* is the maximum interstory drift ratio at all story levels, IDR_i , i=1 to 7. This *EDP* is very well correlated with practically all kinds of structural damage and with many kinds of damage to moment-resisting components. The second type of *EDP* considered was the maximum (peak) absolute floor acceleration at all floor levels, FA_i. This second type of response parameter can be used to estimate the damage to acceleration-sensitive moment-resisting components and building contents.

4.3.1 Assumption 1 — Lognormal Distribution for the *EDP*

Preliminary results, Shome [1999], suggest that the lognormal probability distribution for the probability of occurrence of the maximum interstory drift ratio conditioned on the spectral ordinate at the fundamental period of the structure is a reasonable assumption. However, this assumption typically has been verified for only *IDR* and not for other *EDP*s such as maximum floor accelerations.

Figure 4.1a shows the probability of occurrence of the maximum interstory drift ratio at the first story of the building computed by counting the sorted maximum values in each ground motion scaled to a spectral displacement equal to 20 cm (8 in.). It can be seen that for this level of ground motion intensity there is a factor of nearly four between the minimum and maximum computed values of the peak interstory drift ratio at the first story, showing that the variability of the structural response for a given intensity can be very large. It can be seen that the probability distribution is clearly asymmetric. In order to verify whether a lognormal probability distribution can be assumed, a Kolmogorov-Smirnov goodness-of-fit test [Benjamin and Cornell 1970] was conducted. Also shown in Figure 4.1a is the graphic representation of this test, shown as a K-S test, corresponding to a 90% confidence level. It can be seen that all points, even those near the tails, lie between the limits of acceptability suggesting that, as previously noted by other authors, the lognormal probability distribution assumption is reasonable for this type of engineering demand parameter. The goodness-of-fit test was done at all story levels and at different levels of intensity with similar results.

The same evaluation procedure was applied to maximum absolute floor acceleration at all levels and at different levels of intensity in order to determine whether lognormality can also be assumed for this other type of *edp*. An example is shown in Figure 4.1b for the roof acceleration corresponding to a ground motion intensity level of 20 cm (8 in.). For this level of intensity there is almost a factor of three between the minimum and maximum computed roof acceleration. it can be seen that, even though the fit with the lognormal probability distribution is not as good as that for the interstory drift ratio, still all points lie between the limits of acceptability. Similar results were obtained for other floor levels and other levels of intensity. Hence, it is concluded that the lognormal assumption is also reasonable for maximum floor accelerations.

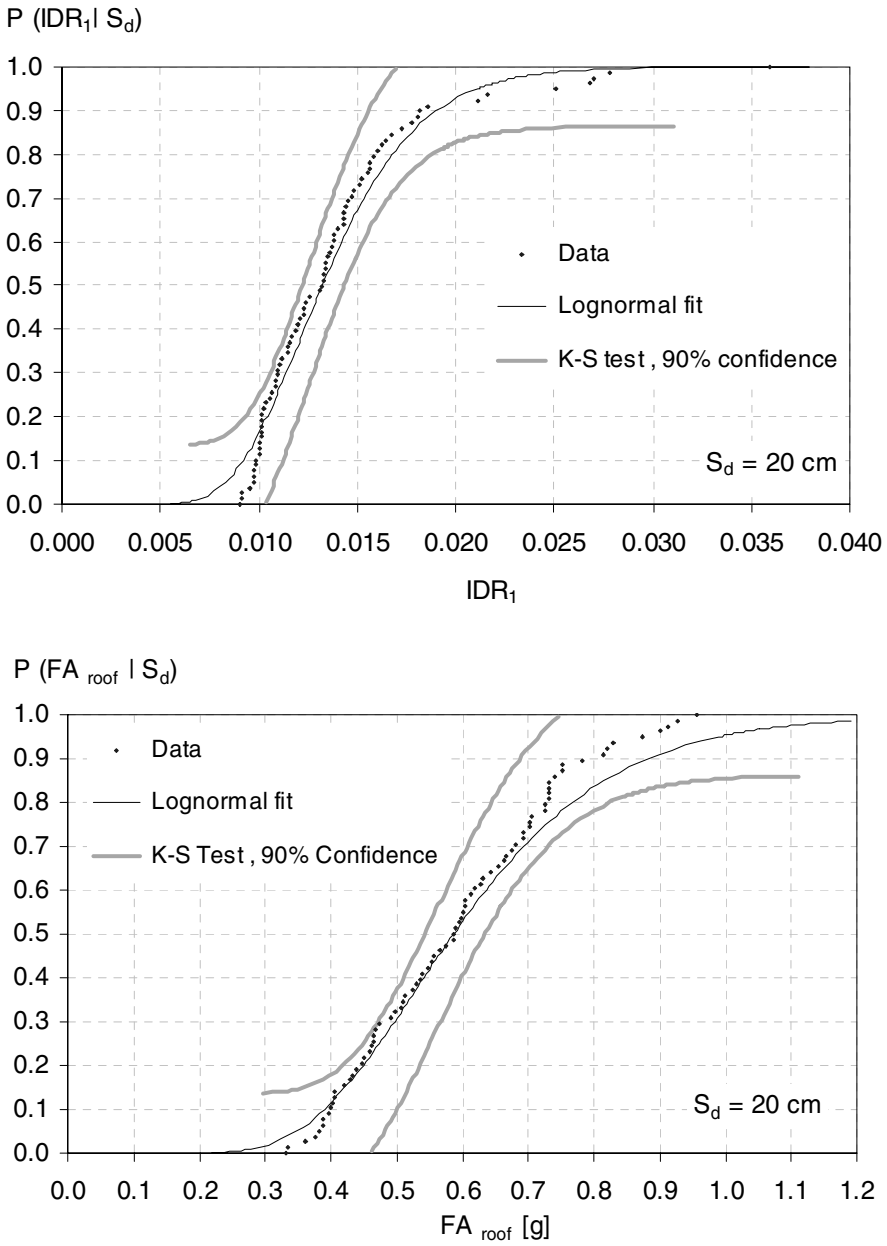

Fig. 4.1 Evaluation of lognormal fit of the conditional probability distribution (a) for first story drift ratio (b) for roof acceleration

4.3.2 Assumption 2 — Simplification of Seismic Hazard Curve

The simplified procedure assumes that the seismic hazard curve has an exponential form and hence becomes linear when plotted in log-log coordinates. In order to approximate the hazard curve using Equation (4.8), the ground motion intensity measure and its corresponding annual

frequency of exceedance at two points are required. The selection of these two points depends primarily on the available seismic hazard data for the site and the range of interest for the levels of intensity. Following the procedure suggested by Luco and Cornell [1998, 1997], the points associated with the probability of occurrence of 10% in 50 years and 2% in 50 years, corresponding to annual frequency of 1/475 and 1/2475 respectively, have been selected in this study to evaluate the constants k_0 and k in Equation (4.8).

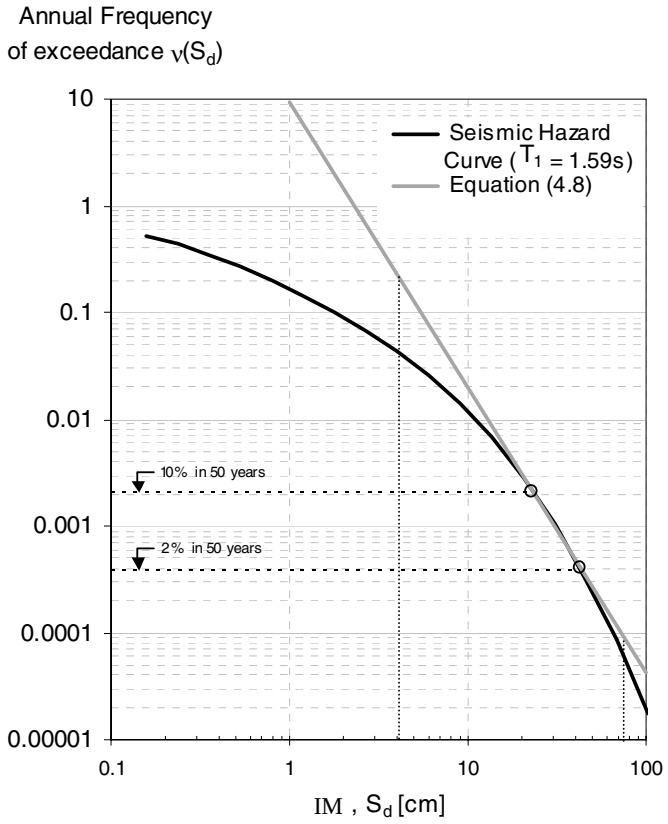

Fig. 4.2 Comparison of seismic hazard curve with that computed with Eq. (4.8)

Figure 4.2 shows the seismic hazard curve corresponding to the site where the building is located in southern California, as computed by the United States Geological Survey, Frankel et al. [2000, 2001]. Here the parameter used to represent the intensity of the ground motion at the site is the spectral displacement of a linear elastic 5% damped single-degree-of-freedom system with a period of vibration equal to the fundamental period of vibration of the building. It can be seen that when plotted in log-log paper this curve is not linear. Kennedy and Short [1994]

suggested that Equation (4.8) could be used over any ten-fold difference in exceedance probabilities, which as shown in this figure, is a reasonable assumption. However, there are situations in which one may be interested in computing a relatively wide range of response quantities which are produced by ground motion intensities associated with more than a ten-fold difference in exceedance probabilities.

This is particularly true in loss estimation where one is interested in ground motions associated with small probabilities of causing damage in a structure to those that have very high probabilities of causing total damage in the structure (total collapse). In these situations, assuming that the seismic hazard curve is linear when plotted in log-log paper may no longer be valid. For example, the range of ground motion intensities that are of interest for this building are marked between the vertical dotted lines in Figure 4.2. This range corresponds to the intensity that has a small probability of triggering moment-resisting damage in the building and the one that has a large probability of producing the collapse of the structure. From this figure it is clear that for this range of ground motion intensities, the linear assumption for the seismic hazard curve is inadequate to approximate the annual rate of exceedance of the ground motion intensity. It should be noted that in the case of more ductile structures the range of interest can be much larger as the structure will be able to undergo significantly larger ground motion intensities without collapse.

4.3.3 Assumption 3 — Variation of Central Tendency of the Response as a Function of Ground Motion Intensity

In order to estimate the conditional probability of the structural response at a given intensity level, using the lognormal distribution, two statistical parameters of the response need to be evaluated as a function of the intensity measure. The first statistical parameter is a central tendency parameter of the response at a given level of intensity. In Equation (4.9) an exponential functional form is used for the estimation of the geometric mean as a function of the level of ground motion intensity. Figure 4.3a compares the variation of the geometric mean of the interstory drift ratio in the first story for different levels of ground motion intensity. It can be seen that even though Equation (4.9) has a relatively good fit, for this particular example at the

first story, it underestimates the median at small levels of intensity and overestimates it at large levels of intensity.

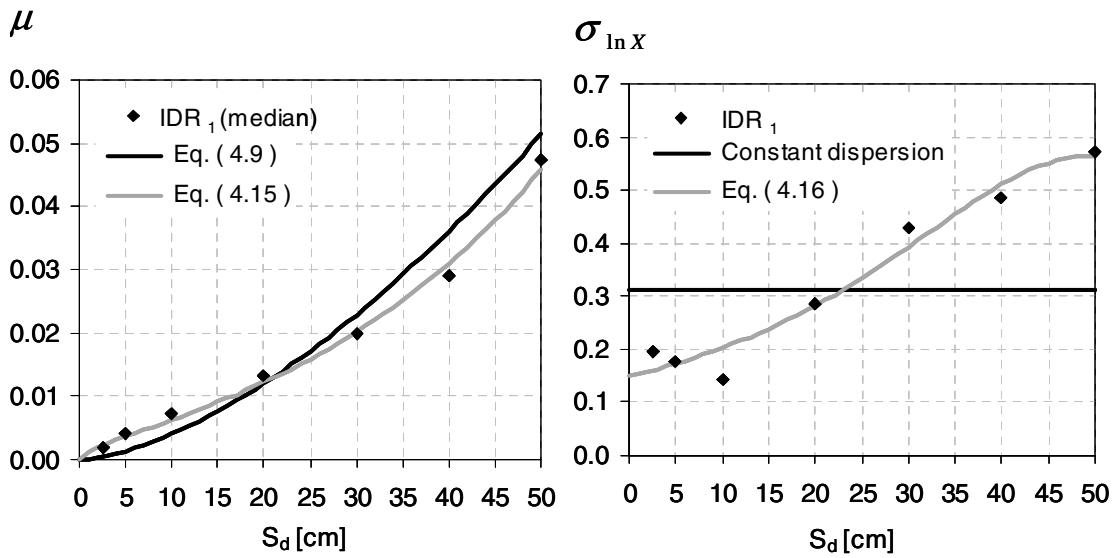

Fig. 4.3 Variation of parameters of the probability distribution of the interstory drift ratio in the first story with changes in the ground motion intensity: (a) median; (b) dispersion

4.3.4 Assumption 4 — Variation of Dispersion as a Function of Loading Intensity

The second required parameter of the conditional probability of the engineering demand parameter is a measure of the dispersion of the structural response at different levels of intensity. Luco and Cornell [1997] recommended a constant global measure of dispersion based on the standard deviation of the natural logarithm of the maximum interstory drift ratio for the range of intensities that are of interest. Figure 4.3b depicts the constant global measure of dispersion compared to the computed dispersion of the interstory drift ratio as a function of the level of intensity. It can be seen that for this range of ground motion intensities the level of dispersion of the interstory drift ratio can change by a factor of four, such that, even if an average constant dispersion is assumed, errors by a factor of two in the level of dispersion can be produced for small and large levels of ground motion intensity.

4.4 PROPOSED APPROACH

4.4.1 Main Considerations

If the seismic hazard curve at the site is available, the most time consuming task in a PSSRA is the estimation of the parameters of the probability distribution of the *EDP*s conditioned to the ground motion intensity, namely the estimation of central tendency and dispersion parameters for various types of *EDP*s at different locations of the structure and for different levels of ground motion intensity. Once parameters k_0, and k have been computed Equation (4.10) allows a fast computation of the annual probability of exceedance of engineering demand parameters. That is, it allows a fast way of solving Equation (4.5). However, solving this integral in most cases represents less than 1% of the effort in this kind of analyses. Hence, there are almost no time-saving benefits in solving Equation (4.5) or (4.6) in closed form.

Based on the above observation, an alternative procedure that can lead to more accurate results is proposed. The main characteristics of the proposed procedure are:

(i) full representation of the seismic hazard curve;

(ii) use of improved parameters to capture the central tendency and the dispersion of the probability distribution of *EDP*s at a given ground motion intensity; and

(iii) use of better functions to represent the variation of the central tendency and the dispersion parameters with changes in the ground motion intensity.

The above improvements are made at the expense of having to numerically integrate Equation (4.5) rather than using a closed-form solution, but practically such numerical integration does not increase the time involved in the PSSRA. The proposed procedure can generically be used for any type of structural response and for any parameter of intensity measure, although here the same parameters previously discussed will be considered.

As shown in Figure 4.2, the exponential form of the seismic hazard curve (i.e., Eq. 4.8) may not yield a good representation of the hazard at the site for all ranges of the ground motion intensity of interest in PBEE. Since in the proposed procedure Equation (4.6) is solved numerically, the actual seismic hazard curve can be used without introducing simplifications. As mentioned in the previous section and exemplified in Figure 4.1, both interstory drift ratios and peak floor accelerations were found to be approximately lognormally distributed; thus, such distribution is adopted in the proposed approach for both types of engineering demand

parameters. It is important to note that making this assumption greatly reduces the number of response history analyses in a PSSRA, as compared for example if a Monte Carlo simulation was used, since the number of analyses required to compute central tendency and dispersion parameters is typically much lower than the one required to compute all the cumulative probability distribution.

4.4.2 Selection of Probability Parameters

The lognormal distribution is fully defined by two parameters: a parameter that describes the central tendency of the random variable and a parameter that describes the dispersion or uncertainty around the central tendency. There is not a unique pair of parameters to fit observed data. Many possible parameters can be used.

A very commonly used central tendency parameter for the lognormal probability distribution is the mean of the natural logarithm of the sample, which is computed as

$$\mu_{\mathrm{Ln}\,x} = \frac{1}{n}\sum_{i=1}^{n} \mathrm{Ln}\; x \tag{4.11}$$

where x is the *EDP* (e.g., interstory drift ratio, peak floor acceleration, etc.) and n is the size of the sample.

Similarly, for describing the dispersion of the random variable a commonly used parameter is the standard deviation of the natural logarithm of the sample data computed as follows

$$\sigma_{\mathrm{Ln}\,x} = \sqrt{\frac{1}{n-1}\sum_{i=1}^{n}(\mathrm{Ln}\; x - \mu_{\mathrm{Ln}\,x})^2} \tag{4.12}$$

The two parameters described by Equations (4.11) and (4.12) are easy to compute and in general produce good estimations of the probability of exceedance of the engineering demand parameter conditioned to a given ground motion intensity level. However, there are situations in which their use can lead to some underestimations or overestimations of the probability of exceedance of the engineering demand parameter. This primarily occurs for large levels of ground motion intensity in which, for certain ground motions, very large engineering demand parameters can be produced that are significantly larger than the rest of the sample. Although

most of the sensitivity of $\mu_{\text{Ln } x}$ to the occurrence of one or a few very large *EDPs*, (values that can be considered outliers) is eliminated by averaging the logarithms of the data, some sensitivity remains that can result in overestimations of the central tendency. However, the overestimation of dispersion can be substantial in the case of $\sigma_{Ln\,x}$ where the differences between the logarithm of individual data points and $\mu_{\text{Ln } x}$ are squared, such that if outliers exist in the sample, they may be large contributors to the summation in Equation (4.12), resulting in an overestimation of the dispersion of the population. To illustrate this potential problem with the use of Equations (4.11) and (4.12), an example corresponding to the interstory drift ratio at the first floor conditioned to the occurrence of spectral displacement of 65 cm is shown in Figure 4.4. It can be seen that the central tendency and particularly the dispersion computed with Equations (4.11) and (4.12) result in overestimation of the parameters that would result in a better fit of most data points in the sample. In particular, using parameters based on these equations leads to underestimations of the probabilities of exceedance of small interstory drift ratios and of overestimating, in some cases by a significant amount, those of large interstory drift ratios. It is important to note that the building used in this paper is probably not capable of sustaining large interstory drifts. Here this intensity level is just used to exemplify the problems that may occur with the use of Equation (4.11) and particularly of Equation (4.12).

A good alternative to Equation (4.11) that is not affected by outliers is to use the counted median of the sample μ, which is obtained very easily by sorting in ascending or descending order the data points. Similarly, a good alternative to Equation (4.12) that is not affected by large individual data points is a dispersion based on the inter-quartile range of the data computed with the following expression [Hoaglin 1983]:

$$\sigma = \frac{P_{75\%} - P_{25\%}}{1.349} \tag{4.13}$$

where $P_{75\%}$ is the 75^{th} percentile of the natural logarithm of the data and $P_{25\%}$ is the 25^{th} percentile of the natural logarithm of the data. The numerator in Equation (4.13) is what is often referred to as the inter-quartile range of the data.

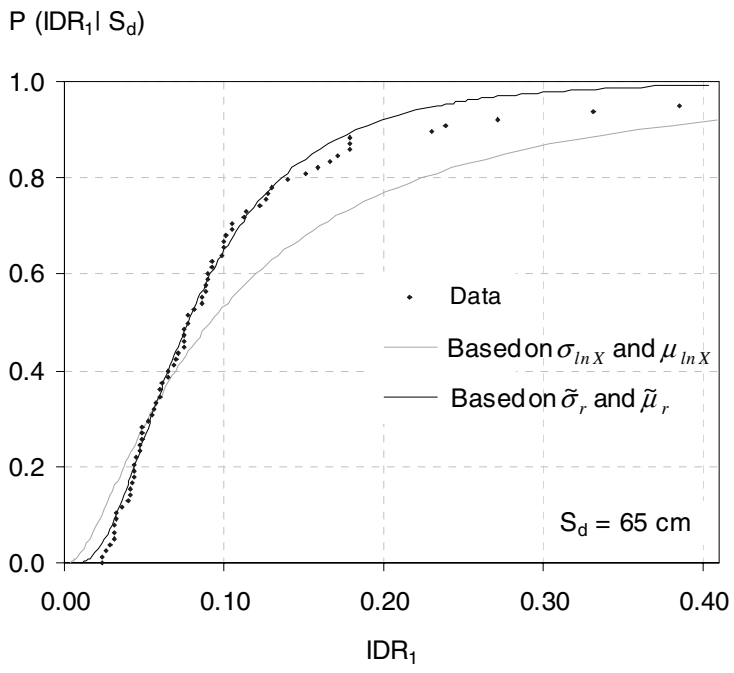

Fig. 4.4 Fitting of the conditional probability distribution with different parameters of the lognormal distribution

In general, the counted median μ and the dispersion parameter σ computed with Equation (4.13) will yield better results than Equations (4.11) and (4.12) as they are not affected by the presence of one or a few data points with very large amplitudes of the engineering demand parameter compared to the rest of the sample. However, these other parameters can also produce some errors in the case of small samples. This is because both the counted median μ and the dispersion parameter σ computed with Equation (4.13) depend on the value of individual data points (1 or 2 in the case of μ and 2 to 4 in the case of σ), so if the sample is small, for example less than 10 data points, then the results of individual response history analyses can lead to underestimations or overestimation of the parameters that would yield a good estimation of the probability distribution of the engineering demand parameter.

Since the response history analyses involved in a PSSRA are the most time-consuming parts of the procedure, it is important to keep the sample size as small as possible. So parameters of central tendency and dispersion that are not affected by the presence of one or a few outliers nor by small sample sizes are preferred in PSSRA.

It can be shown that if the *EDPs* were exactly lognormally distributed then the percentiles of the sample when plotted versus the logarithm of the data would all lie on a straight line. Hence, an improved set of parameters $\tilde{\mu}_r$ and $\tilde{\sigma}_r$ for central tendency and dispersion, to be used in PSSRA is proposed as the ordinate at the origin and slope, respectively, of the line is given by:

$$Ln\ SRP = Ln(\tilde{\mu}_r) + \tilde{\sigma}_r\, \Phi^{-1}[p] \tag{4.14}$$

where p is $\frac{i-1}{n-1}$, Φ^{-1} is the inverse of the standard normal cumulative distribution function. Parameters $\tilde{\mu}_r$ and $\tilde{\sigma}_r$ are computed from a linear regression analyses using as data points Ln *SRP* and $\Phi^{-1}[(i\text{-}1)/(n\text{-}1)]$ of the sorted data that lie in the inter-quartile range. Central tendency and dispersion parameters computed with Equation (4.14) are very robust and in most cases produce very good results. An example of the use of these equations is also shown in Figure 4.4. It can be seen that this approach, although slightly more complicated than Equations (4.11) and (4.12), leads to much better results. Once the parameters on the probability distribution have been computed, the whole probability of exceeding a certain *edp* can be easily computed using Equation (4.3).

4.4.3 Variation of Probability Parameters with Changes in Ground Motion Intensity

Figures 4.5a and 4.6a show variations of central tendency of *EDPs* (computed with Eq. 4.14) with changes in the level of ground motion intensity. Although *EDPs* were computed in all levels of the building, only interstory drift ratios corresponding to the first, fourth and seventh stories and peak floor accelerations corresponding to the second, fifth and eight floors are presented here to illustrate these variations. As shown in these figures median engineering demand parameters typically increase with increasing ground motion intensity. However, the rate of increase changes depending on various factors such as: the type of engineering demand parameter, the location within the structure and the level of ground motion intensity. Furthermore, it can be seen that the rate of increase of the central tendency of the engineering demand parameter in some cases increases and in other decreases as the level of ground motion intensity increases. For example, in Figure 4.5a it can be seen that central tendency of interstory drift ratios in the seventh floor of the building do not grow significantly for ground motions with spectral displacements larger than 30 cm, while in the first story large increases in the median

interstory drift ratio are produced beyond this level of ground motion intensity. Meanwhile for the fourth story the rate of increase of interstory drift ratio with increasing ground motion intensity remains practically constant. In the case of peak floor accelerations, the rate at which this parameter increases with increasing ground motion intensity remains practically constant for the second and fifth floor while this rate decreases in the eighth floor as the ground motion intensity increases.

Dispersions computed with Equation 4.14 at various levels of ground motion intensity are shown in Figures 4.5b and 4.6b for interstory drift ratios and peak floor accelerations, respectively. It can be seen that unlike the central tendency, the dispersions do not necessarily increase with increasing ground motion intensity. For example, while the dispersion of interstory drifts increases in the first and fourth stories as the ground motion intensity increases, in the seventh story the variability of the interstory drift decreases sharply as the ground motion intensity increases. This is the result of concentrations of deformation demands in the lower stories that limit the increase of story deformations in the upper stories for large levels of ground motion intensity. In some cases the variation of dispersion with changes in ground motion intensity can be very complicated showing an increasing trend for low levels of ground motion intensity and a decreasing trend for larger levels of ground motion intensity (e.g., the dispersion on the maximum floor acceleration in the fifth floor).

In a PSSRA it is necessary to obtain simple functions that can capture these variations in the parameters of the probability distribution of *EDPs* while at the same time minimizing the number of parameters in these functions. Complicated variations such as those shown for the dispersion parameter of the maximum floor acceleration in the fifth floor require a minimum of three parameters. Hence, in the proposed procedure three-parameter functions were selected to capture the variation of both the central tendency and dispersion of *EDPs* with changes in ground motion intensity.

The proposed function to represent changes in the central tendency of structural response with changes in ground motion intensity is given by

$$\tilde{\mu}_r = \alpha_1 \alpha_2^{IM} (IM)^{\alpha_3} \tag{4.15}$$

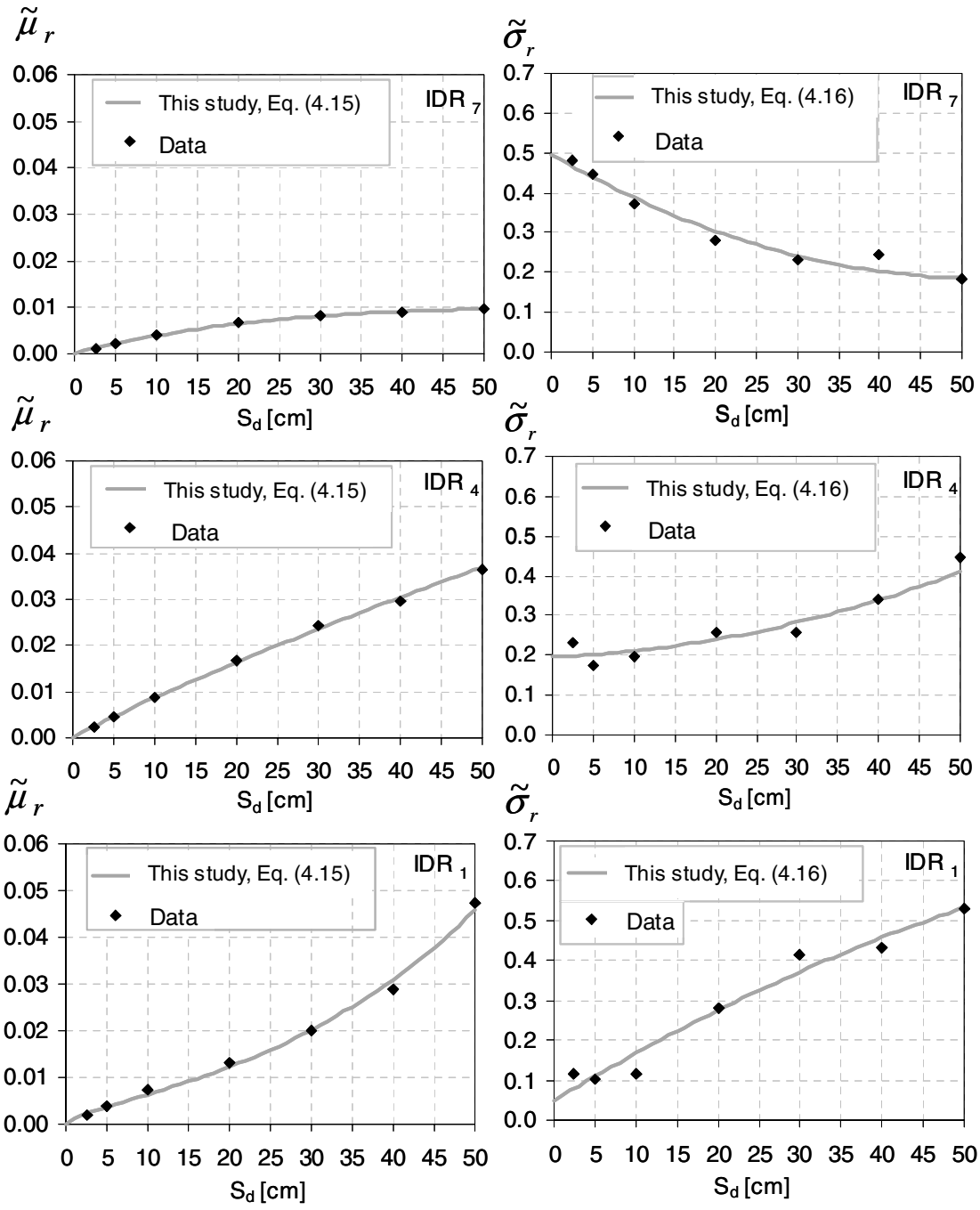

Fig. 4.5 Fitting of parameters of the conditional probability distribution at three stories: (a) central tendency of IDR_i; (b) dispersion of IDR_i

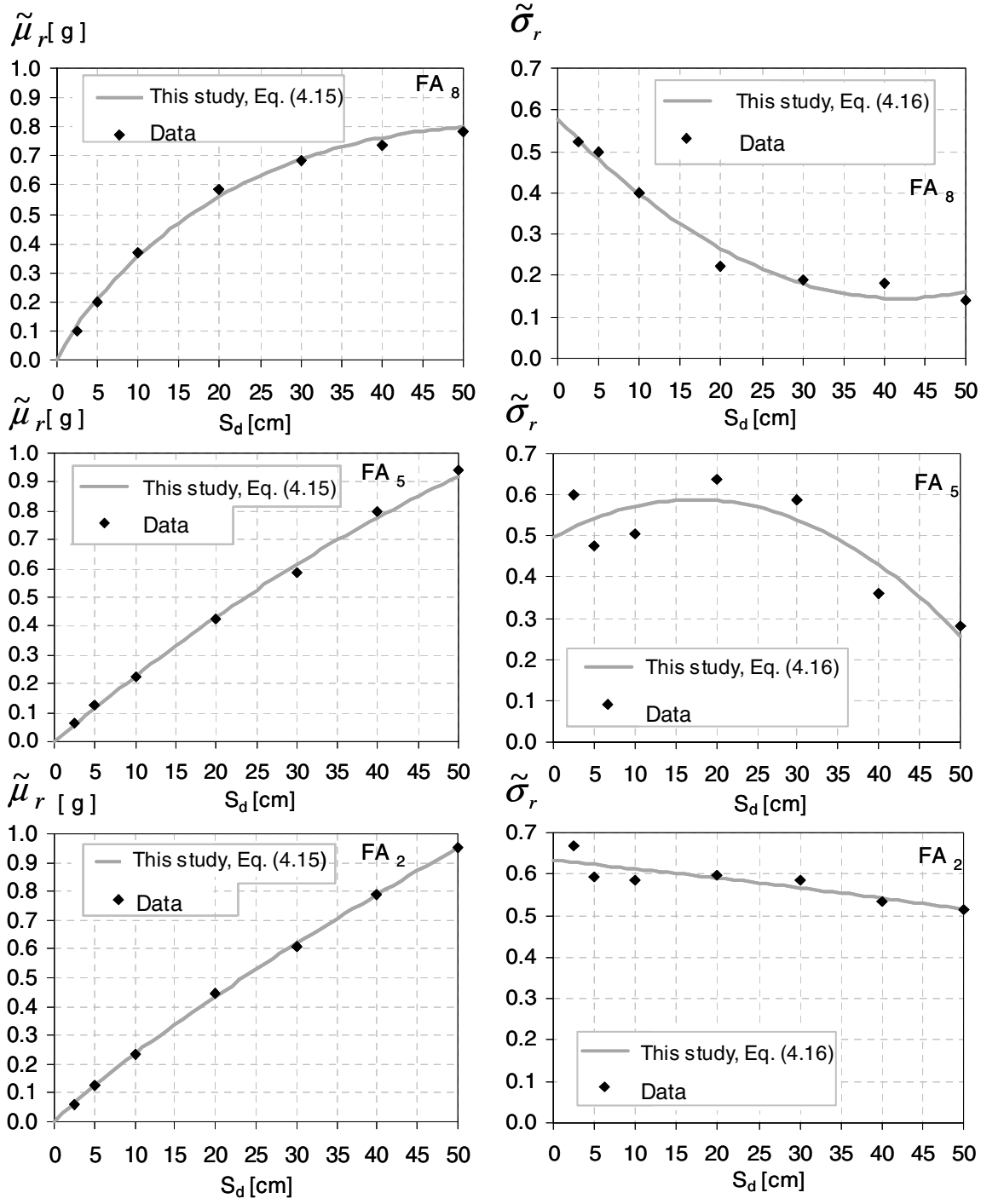

Fig. 4.6 Fitting of parameters of the conditional probability distribution at three floor levels: (a) central tendency of FA_i; (b) dispersion of FA_i

where *IM* is the ground motion intensity measure, and parameters α_1, α_2 , α_3 are constants that are computed from a regression analysis with three known *IM* - $\tilde{\mu}_r$ pairs. The function to represent changes in dispersion of engineering demand parameters with changes in ground motion intensity is given by

$$\tilde{\sigma}_r = \beta_1 + \beta_2 (IM) + \beta_3 (IM)^2 \tag{4.16}$$

where parameters β_1, β_2, and β_3 are constants that are computed from a regression analysis with three known *IM* - $\tilde{\sigma}_r$ pairs. Equations (4.15) and (4.16) are used to represent changes in the parameters of the probability distribution of both interstory drift ratios and peak floor accelerations. The constants, of course will be different depending on the type of engineering demand parameter and the location within the structure.

Figures 4.5 and 4.6 show the fit obtained using Equations (4.15) and (4.16). It can be seen that in most cases these equations capture very well and relatively well the variations of the central tendency and the dispersion, respectively, with changes in the level of ground motion intensity. The use of Equations (4.15) and (4.16) is also shown in Figure 4.3, where it can be seen that these equations provide a significant improvement over those used in the simplified procedure.

Once the variation of parameters of the probability distribution of the *EDPs* has been obtained, it is possible to compute and plot the response parameter at any point in the structure for any given level of ground motion intensity and for any level of conditional probability. An example for interstory drift ratios in the building with 50% (median values) of occurrence conditioned to various levels of ground motion intensity is shown in Figure 4.7a. It can be seen that for low levels of ground motion intensity, the maximum interstory drift occurs at the fifth floor, but as the ground motion intensity increases the location of the maximum interstory drift moves toward the bottom of the building. Furthermore, beyond intensities of 30 cm, very little interstory deformation takes place in the upper two stories. An example for peak floor accelerations and a 75% probability of occurrence is shown in Figure 4.7b. It can be seen that the distribution of accelerations changes significantly with the level of ground motion intensity. At low levels of ground motion intensity, all floors experience similar peak accelerations, whereas at higher levels of ground motion intensity the maximum acceleration in this building are expected to occur at the ground floor.

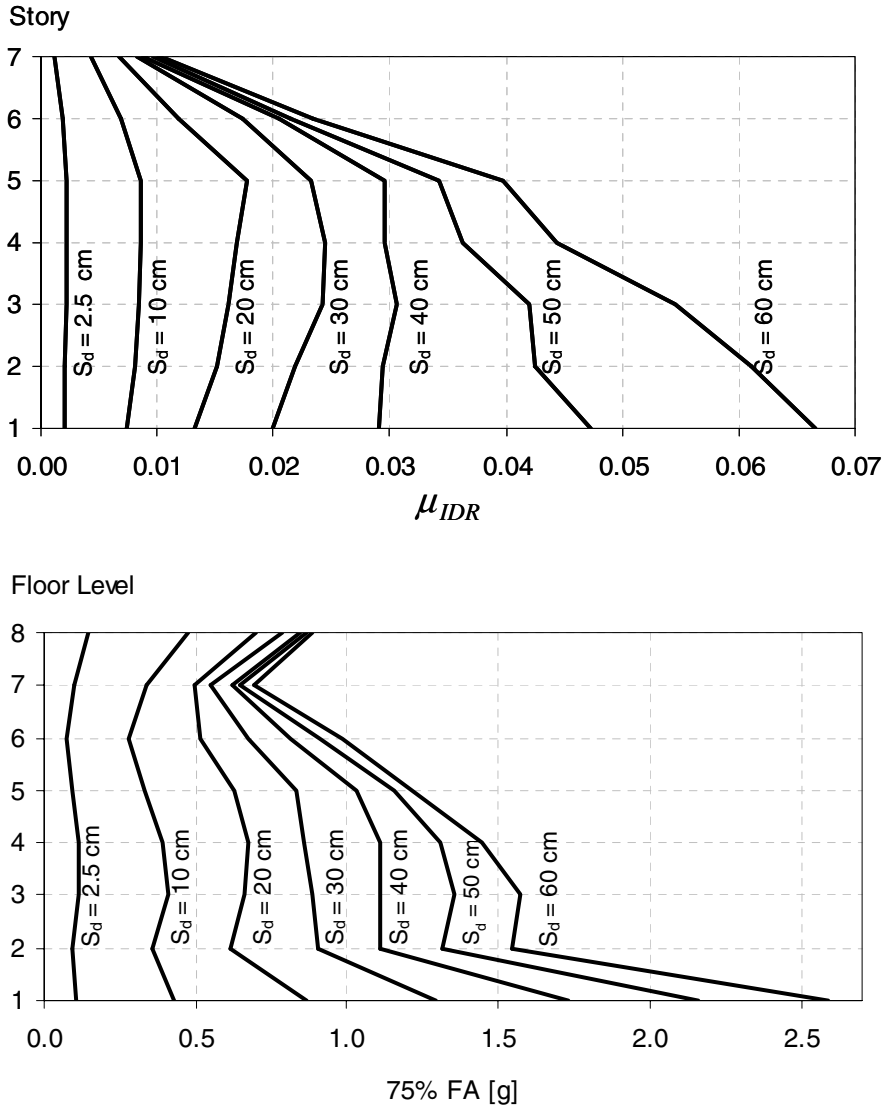

Fig. 4.7 (a) Median of *IDR* at different stories and different levels of intensity; (b) 75th percentile of floor acceleration at different floors and different levels of intensity

4.4.4 Calculation of the Structural Response Probability of Exceedance

Based on the assumptions stated in preceding sections, the probability of the *EDP* exceeding a certain level can be calculated using Equation (4.6). The proposed approach uses the actual seismic hazard curve of the site in Equation (4.6). The approach assumes that the *EDP* at a given level of intensity is lognormally distributed. It is recommended that when more than 20 ground motions are used, the parameter of the central tendency of the conditional probability of *EDP* at

a given level of intensity, $P(EDP < edp \mid IM = im)$, be computed using the sample (counted) median, and when the number of ground motions is smaller than 20, to use the central tendency parameter computed from Equation (4.14). Similarly, when more than 20 ground motions are used, the dispersion parameter can be computed with Equation (4.13), and when the number of ground motions is less than 20, it can be computed using Equation (4.14).

The measures of the central tendency and the dispersion should be calculated at three different levels of ground motion intensity in order to estimate parameters α_1, α_2, and α_3 in Equation (4.15) and parameters β_1, β_2, and β_3 in Equation (4.16). It is recommended that two of these levels of intensity correspond approximately to the limits of the range of interest and the third to approximately the average of the other two intensities.

4.5 EVALUATION OF THE PROCEDURES

4.5.1 Evaluation of the Proposed Procedure

The proposed procedure was used by conducting response history analyses using 40 recorded earthquake ground motions scaled to intensities of 5.0 cm, 30.5 cm, and 61.0 cm (2, 12, and 24 in.). The central tendency and the dispersion parameters were computed for interstory drift ratios at all story levels and of peak floor accelerations at all floor levels in the building using Equation (4.14). The variation of the central tendency and dispersion parameters with changes in ground motion intensity were computed with Equations (4.15) and (4.16). The probability of exceedance of the interstory drift ratios and peak floor accelerations conditioned on ground motion intensity was then computed with Equation (4.7) and finally the probability of exceedance of the interstory drift ratios at all story levels and of peak floor accelerations at all floor levels in the building was calculated with numerical integration of Equation 4.6. Figure 4.8 shows three examples of these results corresponding to the probability of exceedance of interstory drift ratios at the first and seventh stories and the probability of exceedance of the peak floor accelerations at the roof.

In order to evaluate the proposed approach, a more accurate procedure was used to allow for comparison. In this more accurate procedure, referred to here as “exact,” the probability of exceeding a certain response parameter conditioned on a ground motion intensity was obtained by sorting the response computed through nonlinear response history analyses using 79 recorded

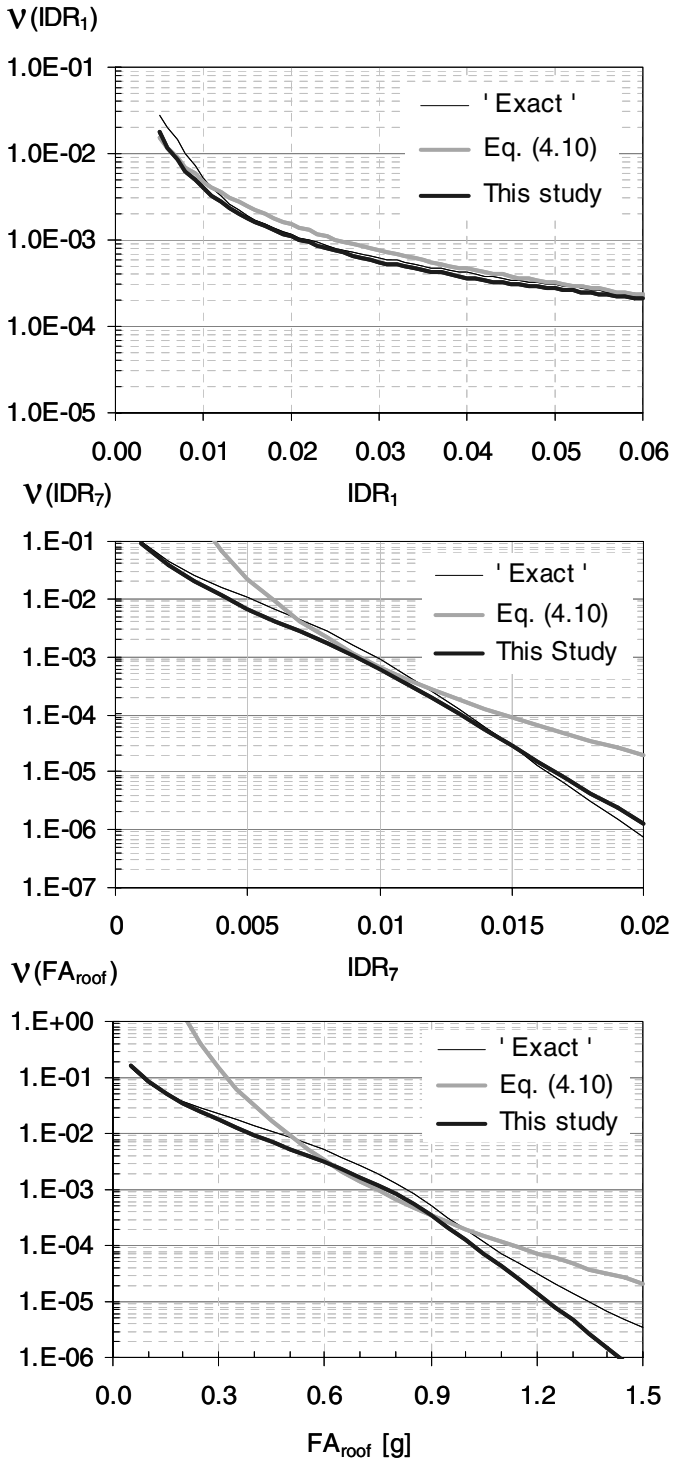

Fig. 4.8 Annual probability of exceedance of the engineering demand parameter. (a) interstory drift ratio in the first story, IDR_1; (b) interstory drift ratio in the seventh story, IDR_7; (c) roof acceleration, FA_{roof}

ground motions scaled to eight different ground motion intensity levels. The number of response history analyses used in the "exact" procedure was 632 as opposed to 120 in the proposed approach. At each of these intensities, percentiles between data points were computed by linear interpolation. Probabilities of exceedance conditioned on ground motion intensity for intensities other than those for which the response history analyses were conducted were computed by using seventh-order polynomials that capture the variation of these probabilities with changes in ground motion intensity. The seventh-order polynomials were obtained by nonlinear regression analyses using the conditional probabilities of building response at each of the eighth ground motion intensities. Probabilities of exceeding engineering demand parameters were then computed with numerical integration of Equation (4.6). The results computed with this "exact" procedure are also shown in Figure 4.8.

As shown in Figure 4.8 the results from the proposed approach, although based on much simpler functions to capture the variation of $P(EDP>edp \mid IM=im)$ with changes in ground motion intensity and using a significantly smaller number of response history analyses, lead to results that are quite similar to those computed using the "exact" procedure. The proposed approach produces small underestimations of results for the interstory drift ratio at the first floor for values smaller than one percent. Similarly small underestimations are produced for interstory drifts at the seventh story and for roof acceleration.

4.5.2 Evaluation of the SAC Procedure

The results computed from the simplified procedure used by Luco and Cornell (Eq. 4.10) to estimate the probability of exceedance of the interstory drift ratio in the first floor of the building are also shown in Figure 4.8a. It can be seen that Equation (4.10) also leads to underestimations for drift ratios smaller than 1%. Similarly, small overestimations are produced for drift ratios between 1% and 5%. There are three main sources of these errors: (a) errors in the estimation of the variation of the central tendency parameter with changes in ground motion intensity; (b) errors in the estimation of the variation of the dispersion parameter with changes in ground motion intensity; and (c) errors due to the approximation of the seismic hazard curve by using Equation (4.8).

In order to identify the effect of each one of these possible sources of error another three analyses were conducted in which each possible source of error was introduced separately and using "exact" results for the other two. In analysis 1 the "exact" central tendency and dispersion parameters were used but the simplified seismic hazard was used. This analysis permits investigating the effect of using Equation (4.8) to approximate the seismic hazard curve. The results of this analysis are shown in Figure 4.9, together with the "exact" results. It can be seen that the approximation in the hazard curve causes a significant overestimation of the annual probability of exceedance of IDR_1 at levels of deformation smaller than 1.5%. At larger levels of deformation, however, this source of approximation does not affect the final probability of exceedance as can be seen in Figure 4.9. In analysis 2 the approximate (constant) dispersion was used in combination with the exact central tendency and the exact seismic hazard curve. This analysis shows the errors introduced by considering the dispersion as constant, that as mentioned before leads to overestimation of dispersion for small ground motion intensities and to overestimations for large ground motion intensities. It can be seen that the approximation in the level of dispersion causes overestimation of the annual probability of exceedance of the response at drift levels smaller than 2.5% and underestimations of the annual probability at drift levels larger than 2.5%. In analysis 3, the approximate central tendency of the interstory drift ratio with changes in intensity measure is used in combination with the exact variation of dispersion and the exact seismic hazard curve. This analysis permits to analyze the effect of using Equation (4.9) to approximate the variation of central tendency. It can be seen that this approximation leads to significant underestimations of the annual probability of exceedance for interstory drifts less than 1.5% and to overestimations for drifts greater than 1.5%. It can be concluded that the main source of difference in the probability of exceedance for drift levels less than 1% observed in Figure 4.8a is produced by the underestimation of the central tendency of the response for ground motion intensities between 2 and 18 cm. However, this error is partially compensated for by the overestimation of the seismic hazard curve and by the overestimation of dispersion at small levels of intensity.

Although it is possible to find many situations in which the three main approximations in Equation (4.10) lead to small errors or to larger errors that partially compensate for each other, there are other situations in which the use of this equation can lead to significant errors, especially when used in combination with a wide range of ground motion intensities. Figure 4.8b compares the results computed with Equation (4.10) to "exact" results for the interstory drift

ratio in the seventh floor. It can be seen that for drift ratios less than 0.7% and for drift ratios greater than 1.2% the probability of exceedance computed with the simplified approach for the seventh floor is much larger than the one calculated with the "exact" approach. For example, the probability of the seventh story drift ratio exceeding 0.35% computed with Equation (4.10) is approximately five times greater than the one calculated with the "exact" approach. This large difference is produced by an overestimation of the central tendency and of the seismic hazard curve for small levels of ground motion intensity.

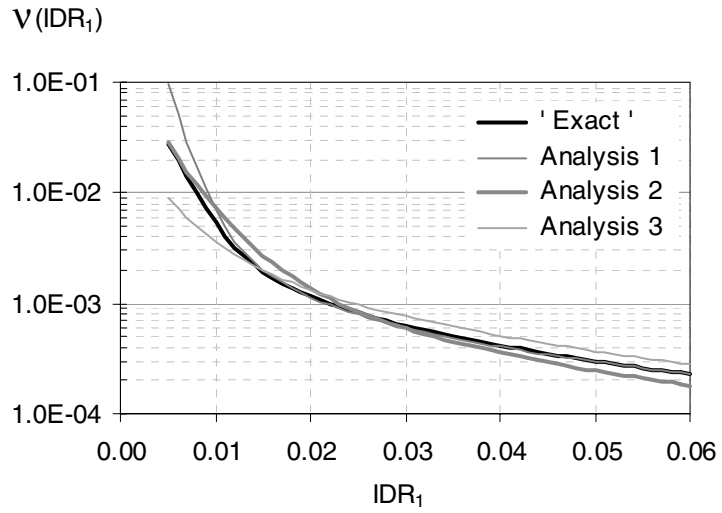

Fig. 4.9 Effects of the three simplifying assumptions on the annual probability of exceedance of the interstory drift ratio in the first story, IDR_1.

Figure 4.8c provides a comparison between the probability of exceedance of roof accelerations computed with Equation (4.10) and the one calculated with the "exact" procedure. As seen in this figure, for floor accelerations less than 0.5g and greater than 1g the results computed with Equation (4.10) are larger and in some cases much larger than those of the "exact" results. For example, the probability of roof acceleration exceeding 0.25g, computed with Equation (4.10) is more than one order of magnitude larger than the one calculated with the "exact" procedure. The probability of exceeding an acceleration of 1.5g at the roof computed with simplified approach is 6 times larger than the "exact" one.

5 Summary of Procedure to Estimate Probabilistic Building Response

The procedure presented in this study is generic and can be used for many types of engineering demand parameters for a facility. The following steps need to be accomplished in order to estimate the probability of exceedance of the engineering demand parameter:

1. Develop a realistic model of the structure for the nonlinear response history analyses.
2. Select a suite of earthquake ground motion time histories. The size of the suite of earthquake ground motions is a function of the performance level of interest and the *EDP* for which the probability of exceedance is being computed. At this point we recommend a size of 30 ground motions for a robust estimate of the probability of exceedance for the interstory drift ratio and the peak floor acceleration.
3. Select an intensity measure. An elastic spectral ordinate is an appropriate intensity measure for many buildings. For structures that are capable of sustaining highly nonlinear deformations, the inelastic spectral ordinate might be a better intensity measure.
4. Scale the suite of earthquake ground motions based on the selected intensity measure.
5. Apply the scaled suite of earthquake time histories to the model at three different levels of intensity to estimate the structural response of interest at those three levels of intensity. We recommend one low level of intensity, one high level of intensity, and one level of intensity in between. Simplified analyses techniques can be used to obtain rough estimates of building response to selecting these levels of intensities.
6. Compute the probability parameters of the *EDP*, central tendency and dispersion, at those three levels of intensity, using the procedure described in section 4.4.2.

7. Compute the variations of the central tendency and the dispersion of the *EDP* with the levels of intensity using Equations (4.15) and (4.16), respectively.
8. Compute the probability of exceedance of the engineering demand parameter at different levels, using Equation (4.6) and applying a numerical integration.

6 Conclusions

A methodology to evaluate economic losses in buildings was presented. A primary step in the methodology is to estimate the structural response of the building in a probabilistic framework. A procedure to estimate the probability of exceedance of structural response has been presented. The proposed procedure is quite generic and can be used for the probability of exceedance of any type of *EDP*. The procedure combines the probability of exceedance of the structural response conditioned on the ground motion intensity with the seismic hazard curve at the site. The probability of exceedance of structural response conditioned on the ground motion intensity is computed by assuming a lognormal distribution and by using parameters to estimate the central tendency and dispersion at a given level of intensity, together with simple equations that capture the variation of these parameters with changes in ground motion intensity. It was verified by assuming that the lognormal distribution is not only valid for the maximum interstory drift in the building but also for the maximum drift at any level in the building and also for peak floor accelerations.

Various measures of the central tendency and dispersion to be used as parameters for the lognormal distribution were evaluated. The first and most commonly used alternative is the use of mean and standard deviation of the natural logarithm of the response as measures of the central tendency and dispersion, respectively. It was shown that these parameters can lead to overestimation or underestimation of the probability of exceedance of the structural response parameter when the ground motion intensity is large, where very large responses may be computed with certain ground motions. A second alternative is to use the sample median as a measure of central tendency and a measure of dispersion derived from the inter-quartile range of the data. These two alternative parameters, although capable of producing better results than the first alternative, can also lead to errors in the probability of exceedance of the structural response conditioned on ground motion intensity, particularly when the number of ground motions is small. Therefore, a third alternative to calculate measures of the central tendency and dispersion

has been proposed. This alternative, which is based on a linear regression analysis of the results in the normal probability paper, leads to very robust parameter estimation, particularly when the sample size is small.

The accuracy of the proposed approach and of the closed-form procedure have been evaluated for three engineering demand parameters, by comparing their results with "exact" results. The "exact" results were computed using a relatively large number of ground motions scaled at eight different levels of ground motion intensity. The variation of probability of exceedance of building response with changes in ground motion intensity was computed with seventh-order polynomials that capture very accurately this variation. It is concluded that the proposed approach leads to very good results that are much closer to the "exact" results than those produced by the simplified closed-form procedure. In some cases, the simplified closed-form procedure leads to relatively good results. However, in other cases, the errors can be substantial. In particular, it was found that assuming that the seismic hazard curve is linear in log-log paper and that the dispersion remains constant with changes in ground motion intensity can lead to significant errors when a wide range of structural response, produced by a wide range of ground motion intensities, is of interest.

REFERENCES

Bazzuro, P. and Cornell, C.A. (1994). Seismic hazard analysis for non-linear structures. I: Methodology, ASCE, *J. Struct. Engrg.,* 120(11): 3320-3344.

Bazzuro, P. and Cornell, C.A. (1994). Seismic hazard analysis for non-linear structures. II: Applications, ASCE, *J. Struct. Engrg.,* 120(11): 3345-3365.

Benjamin, J. and Cornell, C.A. (1970). *Probability, Statistics, and Decision for Civil Engineers,* McGraw-Hill, New York.

Bertero, V.V. (1977). Strength and deformation capacities of buildings under extreme environments, *Struc. Engrg. and Struc. Mchncs.*, Pister K.S. (ed), Prentice Hall, New Jersey: 211-215.

Blume, J. A. and Associates. (1973). Holiday Inn, San Fernando, California, Earthquake of February 9, 1971, U.S. Department of Commerce, National Oceanic and Atmospheric Administration, Washington, DC: 395 – 422.

Browning, J., Li, R., Lynn, A., and Moehle, J. P. (2000). Performance Assessment for a Reinforced Concrete Frame Building, Earthquake Spectra, 16(3): 541-555.

Cornell, C. A. (1996). Calculating building seismic performance reliability: a basis for multi-level design norms, *Proc.*, 11th World Conf. on Earthq. Engrg., Pergamon, Elsevier Science Ltd., [Oxford, England].

Esteva, L. (1980). *Design: General, in Design of earthquake resistant structures*, Ed. E. Rosenblueth, Pentech Press Ltd., Plymouth, Great Britain: 54-99.

Frankel, A. D, Leyendecker E. V. and Harmsen S. C. (2000). Conveying seismic hazard information to engineers, *Proc.,* International Conference on Seismic Zonation: Managing Earthquake Risk in the 21st Century, Earthquake Engineering Research Inst., Oakland, Calif.

Frankel, A. D. and Leyendecker, E. V. (2001). Seismic Hazard Curves and Uniform Hazard Response Spectra for the United States, Version 3.01. United States Geological Survey, Denver, Co.

Hoaglin, D.C., Mosteller, F. and Tukey, J.W. (1983). Understanding robust and exploratory data analysis. John Wiley & Sons Inc.: New York.

Hwang, S. J. and Moehle, J. P. (1993). An experimental study of flat-plate structures under vertical and lateral loads, UCB/EERC-93/03, Berkeley, California.

John A. Blume & Associates. (1971). *Report on Holliday Inn, San Fernando, California, Earthquake of February 9,1971,* U.S. Department of Commerce, National Oceanic and Atmospheric Administration: 359-393.

Kennedy, R.C. and Short, S. A. (1994). Basis for seismic provisions of DOE-STD-1020, Report UCRL-CR-111478, S/C - B235302, Brookhaven Natl. Lab. BNL-52418, Lawrence Livermore National Lab.

Luco, N. and Cornell, C.A. (1997). Numerical example of the proposed SAC procedure for assessing the annual exceedance probabilities of specified drift demands and of drift capacity, Internal SAC report.

Luco, N. and Cornell, C.A. (1998). Effects of random connection fractures on demands and reliability for a 3-story pre-Northridge SMRF structure, *Proc.*, 6th U.S. Nat. Conf. on Earthq. Engrg., Seattle, Washington.

Luco, N. and Cornell, C.A. (2000). Effects of connection fractures on SMRF seismic drift demands, *ASCE, J. Struc. Engrg.,* 126(1): 127-136.

Medina, R. and Krawinkler, H. (2001). Seismic demands for performance-based design. *Proc., First PEER annual meeting*, Oakland, California.

Mehanny, S.S. and Deierlein, G.G. (2000). Modeling and assessment of seismic performance of composite frames with reinforced concrete columns and steel beams, *Report No. 136*, The John A. Blume Earthquake Engineering Center, Stanford University, Stanford.

Miranda, E. (1993). Site-dependent strength reduction factors. *ASCE, J. Struc. Engrg.* 119(12): 3503- 3519.

Miranda, E. (1991). Seismic evaluation and upgrading of existing buildings, Ph.D. thesis, Univ. of California at Berkeley : 482 pages.

Miranda, E. (1997). Strength reduction factors in performance-based design, *The EERC – CUREe Symposium in honor of Vitelmo V. Bertero.* UCB / EERC – 97 / 05, Berkeley, California: 125-132.

Miranda, E. (2000). Inelastic displacement ratios for structures on firm sites, *ASCE, J. Struc. Engrg.*, 126(10): 1150-1159

Miranda, E. and Aslani, H. (2001). Probabilistic estimation of building response for performance-based engineering, *Proc. 4th US-Japan Workshop on Performance Based Earthquake Engineering of RC Structures*, Seattle, Washington.

Miranda E, Aslani H. Probabilistic building response assessment. *ASCE, J. Struc. Engrg.* (submitted).

Naeim, F. (1997). Seismic Performance of Instrumented Buildings – An Interactive CD-ROM Based Information System, A Report to California Division of Mines and Geology, Strong Motion Instrumentation Program, In preparation.

Ordaz, M., Miranda, E., Reinoso, E. and Perez-Rocha LE. (2000). Seismic loss estimation model for Mexico City, *Proc*., 12th World Conf. on Earthq. Engrg., Auckland, New Zealand.

Santa-Ana, P.R. and Miranda, E. (2000). Strength reduction factors for multi-degree of freedom systems. *Proc.* 12th World Conference on Earthq. Engrg. Auckland, New Zealand.

Sewell, R.T. (1989). Damage effectiveness of earthquake ground motion: Characterizations based on the performance of structures and equipment, Stanford University, Stanford.

Shome, N., Cornell, C.A. (1999). Probabilistic seismic demand analysis of nonlinear structures, *Report RMS-35*, Reliability of Marine Structures Program, Stanford University, Stanford.

Vamvatsikos, D. and Cornell, C.A. (2002). Incremental Dynamic Analysis, *Earthq. Engrg and Struc. Dyn.,* 31(3): 491-514.

Yun, S.Y., Hamburger, R.O., Cornell, C.A. and Foutch, D.A. (2002). Seismic performance for steel moment frames. *ASCE., J. of Struc. Engrg.,* 128(4): 534-545.

PEER REPORTS

PEER reports are available from the National Information Service for Earthquake Engineering (NISEE). To order PEER reports, please contact the Pacific Earthquake Engineering Research Center, 1301 South 46th Street, Richmond, California 94804-4698. Tel.: (510) 231-9468; Fax: (510) 231-9461.

PEER 2003/06 *Performance of Circular Reinforced Concrete Bridge Columns under Bidirectional Earthquake Loading.* Mahmoud M. Hachem, Stephen A. Mahin, and Jack P. Moehle. February 2003.

PEER 2003/03 *Probabilistic Response Assessment for Building-Specific Loss Estimation.* Eduardo Miranda and Hesameddin Aslani. September 2003.

PEER 2003/02 *Software Framework for Collaborative Development of Nonlinear Dynamic Analysis Program.* Jun Peng and Kincho H. Law. September 2003.

PEER 2002/24 *Performance of Beam to Column Bridge Joints Subjected to a Large Velocity Pulse.* Natalie Gibson, André Filiatrault, and Scott A. Ashford. April 2002.

PEER 2002/23 *Effects of Large Velocity Pulses on Reinforced Concrete Bridge Columns.* Greg L. Orozco and Scott A. Ashford. April 2002.

PEER 2002/22 *Characterization of Large Velocity Pulses for Laboratory Testing.* Kenneth E. Cox and Scott A. Ashford. April 2002.

PEER 2002/21 *Fourth U.S.-Japan Workshop on Performance-Based Earthquake Engineering Methodology for Reinforced Concrete Building Structures*. December 2002.

PEER 2002/20 *Barriers to Adoption and Implementation of PBEE Innovations.* Peter J. May. August 2002.

PEER 2002/19 *Economic-Engineered Integrated Models for Earthquakes: Socioeconomic Impacts.* Peter Gordon, James E. Moore II, and Harry W. Richardson. July 2002.

PEER 2002/18 *Assessment of Reinforced Concrete Building Exterior Joints with Substandard Details.* Chris P. Pantelides, Jon Hansen, Justin Nadauld, and Lawrence D. Reaveley. May 2002.

PEER 2002/17 *Structural Characterization and Seismic Response Analysis of a Highway Overcrossing Equipped with Elastomeric Bearings and Fluid Dampers: A Case Study.* Nicos Makris and Jian Zhang. November 2002.

PEER 2002/16 *Estimation of Uncertainty in Geotechnical Properties for Performance-Based Earthquake Engineering.* Allen L. Jones, Steven L. Kramer, and Pedro Arduino. December 2002.

PEER 2002/15 *Seismic Behavior of Bridge Columns Subjected to Various Loading Patterns.* Asadollah Esmaeily-Gh. and Yan Xiao. December 2002.

PEER 2002/14 *Inelastic Seismic Response of Extended Pile Shaft Supported Bridge Structures.* T.C. Hutchinson, R.W. Boulanger, Y.H. Chai, and I.M. Idriss. December 2002.

PEER 2002/13 *Probabilistic Models and Fragility Estimates for Bridge Components and Systems.* Paolo Gardoni, Armen Der Kiureghian, and Khalid M. Mosalam. June 2002.

PEER 2002/12 *Effects of Fault Dip and Slip Rake on Near-Source Ground Motions: Why Chi-Chi Was a Relatively Mild M7.6 Earthquake.* Brad T. Aagaard, John F. Hall, and Thomas H. Heaton. December 2002.

PEER 2002/11 *Analytical and Experimental Study of Fiber-Reinforced Strip Isolators*. James M. Kelly and Shakhzod M. Takhirov. September 2002.

PEER 2002/10 *Centrifuge Modeling of Settlement and Lateral Spreading with Comparisons to Numerical Analyses***.** Sivapalan Gajan and Bruce L. Kutter. January 2003.

PEER 2002/09 *Documentation and Analysis of Field Case Histories of Seismic Compression during the 1994 Northridge, California, Earthquake.* Jonathan P. Stewart, Patrick M. Smith, Daniel H. Whang, and Jonathan D. Bray. October 2002.

PEER 2002/08 *Component Testing, Stability Analysis and Characterization of Buckling-Restrained Unbonded Braces™.* Cameron Black, Nicos Makris, and Ian Aiken. September 2002.

PEER 2002/07 *Seismic Performance of Pile-Wharf Connections.* Charles W. Roeder, Robert Graff, Jennifer Soderstrom, and Jun Han Yoo. December 2001.

PEER 2002/06 *The Use of Benefit-Cost Analysis for Evaluation of Performance-Based Earthquake Engineering Decisions*. Richard O. Zerbe and Anthony Falit-Baiamonte. September 2001.

PEER 2002/05 *Guidelines, Specifications, and Seismic Performance Characterization of Nonstructural Building Components and Equipment*. André Filiatrault, Constantin Christopoulos, and Christopher Stearns. September 2001.

PEER 2002/04 *Consortium of Organizations for Strong-Motion Observation Systems and the Pacific Earthquake Engineering Research Center Lifelines Program: Invited Workshop on Archiving and Web Dissemination of Geotechnical Data, 4–5 October 2001*. September 2002.

PEER 2002/03 *Investigation of Sensitivity of Building Loss Estimates to Major Uncertain Variables for the Van Nuys Testbed.* Keith A. Porter, James L. Beck, and Rustem V. Shaikhutdinov. August 2002.

PEER 2002/02 *The Third U.S.-Japan Workshop on Performance-Based Earthquake Engineering Methodology for Reinforced Concrete Building Structures*. July 2002.

PEER 2002/01 *Nonstructural Loss Estimation: The UC Berkeley Case Study. Mary C. Comerio and John C. Stallmeyer.* December 2001.

PEER 2001/16 *Statistics of SDF-System Estimate of Roof Displacement for Pushover Analysis of Buildings.* Anil K. Chopra, Rakesh K. Goel, and Chatpan Chintanapakdee. December 2001.

PEER 2001/15 *Damage to Bridges during the 2001 Nisqually Earthquake.* R. Tyler Ranf, Marc O. Eberhard, and Michael P. Berry. November 2001.

PEER 2001/14 *Rocking Response of Equipment Anchored to a Base Foundation.* Nicos Makris and Cameron J. Black. September 2001.

PEER 2001/13 *Modeling Soil Liquefaction Hazards for Performance-Based Earthquake Engineering.* Steven L. Kramer and Ahmed-W. Elgamal. February 2001.

PEER 2001/12 *Development of Geotechnical Capabilities in OpenSees.* Boris Jeremic. September 2001.

PEER 2001/11 *Analytical and Experimental Study of Fiber-Reinforced Elastomeric Isolators*. James M. Kelly and Shakhzod M. Takhirov. September 2001.

PEER 2001/10 *Amplification Factors for Spectral Acceleration in Active Regions.* Jonathan P. Stewart, Andrew H. Liu, Yoojoong Choi, and Mehmet B. Baturay. December 2001.

PEER 2001/09 *Ground Motion Evaluation Procedures for Performance-Based Design.* Jonathan P. Stewart, Shyh-Jeng Chiou, Jonathan D. Bray, Robert W. Graves, Paul G. Somerville, and Norman A. Abrahamson. September 2001.

PEER 2001/08 *Experimental and Computational Evaluation of Reinforced Concrete Bridge Beam-Column Connections for Seismic Performance*. Clay J. Naito, Jack P. Moehle, and Khalid M. Mosalam. November 2001.

PEER 2001/07 *The Rocking Spectrum and the Shortcomings of Design Guidelines.* Nicos Makris and Dimitrios Konstantinidis. August 2001.

PEER 2001/06 *Development of an Electrical Substation Equipment Performance Database for Evaluation of Equipment Fragilities*. Thalia Agnanos. April 1999.

PEER 2001/05 *Stiffness Analysis of Fiber-Reinforced Elastomeric Isolators.* Hsiang-Chuan Tsai and James M. Kelly. May 2001.

PEER 2001/04 *Organizational and Societal Considerations for Performance-Based Earthquake Engineering.* Peter J. May. April 2001.

PEER 2001/03 *A Modal Pushover Analysis Procedure to Estimate Seismic Demands for Buildings: Theory and Preliminary Evaluation.* Anil K. Chopra and Rakesh K. Goel. January 2001.

PEER 2001/02 *Seismic Response Analysis of Highway Overcrossings Including Soil-Structure Interaction.* Jian Zhang and Nicos Makris. March 2001.

PEER 2001/01 *Experimental Study of Large Seismic Steel Beam-to-Column Connections.* Egor P. Popov and Shakhzod M. Takhirov. November 2000.

PEER 2000/10 *The Second U.S.-Japan Workshop on Performance-Based Earthquake Engineering Methodology for Reinforced Concrete Building Structures.* March 2000.

PEER 2000/09 *Structural Engineering Reconnaissance of the August 17, 1999 Earthquake: Kocaeli (Izmit), Turkey.* Halil Sezen, Kenneth J. Elwood, Andrew S. Whittaker, Khalid Mosalam, John J. Wallace, and John F. Stanton. December 2000.

PEER 2000/08 *Behavior of Reinforced Concrete Bridge Columns Having Varying Aspect Ratios and Varying Lengths of Confinement.* Anthony J. Calderone, Dawn E. Lehman, and Jack P. Moehle. January 2001.

PEER 2000/07 *Cover-Plate and Flange-Plate Reinforced Steel Moment-Resisting Connections.* Taejin Kim, Andrew S. Whittaker, Amir S. Gilani, Vitelmo V. Bertero, and Shakhzod M. Takhirov. September 2000.

PEER 2000/06 *Seismic Evaluation and Analysis of 230-kV Disconnect Switches.* Amir S. J. Gilani, Andrew S. Whittaker, Gregory L. Fenves, Chun-Hao Chen, Henry Ho, and Eric Fujisaki. July 2000.

PEER 2000/05 *Performance-Based Evaluation of Exterior Reinforced Concrete Building Joints for Seismic Excitation.* Chandra Clyde, Chris P. Pantelides, and Lawrence D. Reaveley. July 2000.

PEER 2000/04 *An Evaluation of Seismic Energy Demand: An Attenuation Approach.* Chung-Che Chou and Chia-Ming Uang. July 1999.

PEER 2000/03 *Framing Earthquake Retrofitting Decisions: The Case of Hillside Homes in Los Angeles.* Detlof von Winterfeldt, Nels Roselund, and Alicia Kitsuse. March 2000.

PEER 2000/02 *U.S.-Japan Workshop on the Effects of Near-Field Earthquake Shaking.* Andrew Whittaker, ed. July 2000.

PEER 2000/01 *Further Studies on Seismic Interaction in Interconnected Electrical Substation Equipment.* Armen Der Kiureghian, Kee-Jeung Hong, and Jerome L. Sackman. November 1999.

PEER 1999/14 *Seismic Evaluation and Retrofit of 230-kV Porcelain Transformer Bushings*. Amir S. Gilani, Andrew S. Whittaker, Gregory L. Fenves, and Eric Fujisaki. December 1999.

PEER 1999/13 *Building Vulnerability Studies: Modeling and Evaluation of Tilt-up and Steel Reinforced Concrete Buildings.* John W. Wallace, Jonathan P. Stewart, and Andrew S. Whittaker, editors. December 1999.

PEER 1999/12 *Rehabilitation of Nonductile RC Frame Building Using Encasement Plates and Energy-Dissipating Devices.* Mehrdad Sasani, Vitelmo V. Bertero, James C. Anderson. December 1999.

PEER 1999/11 *Performance Evaluation Database for Concrete Bridge Components and Systems under Simulated Seismic Loads.* Yael D. Hose and Frieder Seible. November 1999.

PEER 1999/10 *U.S.-Japan Workshop on Performance-Based Earthquake Engineering Methodology for Reinforced Concrete Building Structures.* December 1999.

PEER 1999/09 *Performance Improvement of Long Period Building Structures Subjected to Severe Pulse-Type Ground Motions*. James C. Anderson, Vitelmo V. Bertero, and Raul Bertero. October 1999.

PEER 1999/08 *Envelopes for Seismic Response Vectors.* Charles Menun and Armen Der Kiureghian. July 1999.

PEER 1999/07 *Documentation of Strengths and Weaknesses of Current Computer Analysis Methods for Seismic Performance of Reinforced Concrete Members.* William F. Cofer. November 1999.

PEER 1999/06 *Rocking Response and Overturning of Anchored Equipment under Seismic Excitations.* Nicos Makris and Jian Zhang. November 1999.

PEER 1999/05 *Seismic Evaluation of 550 kV Porcelain Transformer Bushings.* Amir S. Gilani, Andrew S. Whittaker, Gregory L. Fenves, and Eric Fujisaki. October 1999.

PEER 1999/04 *Adoption and Enforcement of Earthquake Risk-Reduction Measures.* Peter J. May, Raymond J. Burby, T. Jens Feeley, and Robert Wood.

PEER 1999/03 *Task 3 Characterization of Site Response General Site Categories*. Adrian Rodriguez-Marek, Jonathan D. Bray, and Norman Abrahamson. February 1999.

PEER 1999/02 *Capacity-Demand-Diagram Methods for Estimating Seismic Deformation of Inelastic Structures: SDF Systems*. Anil K. Chopra and Rakesh Goel. April 1999.

PEER 1999/01 *Interaction in Interconnected Electrical Substation Equipment Subjected to Earthquake Ground Motions.* Armen Der Kiureghian, Jerome L. Sackman, and Kee-Jeung Hong. February 1999.

PEER 1998/08 *Behavior and Failure Analysis of a Multiple-Frame Highway Bridge in the 1994 Northridge Earthquake.* Gregory L. Fenves and Michael Ellery. December 1998.

PEER 1998/07 *Empirical Evaluation of Inertial Soil-Structure Interaction Effects.* Jonathan P. Stewart, Raymond B. Seed, and Gregory L. Fenves. November 1998.

PEER 1998/06 *Effect of Damping Mechanisms on the Response of Seismic Isolated Structures.* Nicos Makris and Shih-Po Chang. November 1998.

PEER 1998/05 *Rocking Response and Overturning of Equipment under Horizontal Pulse-Type Motions.* Nicos Makris and Yiannis Roussos. October 1998.

PEER 1998/04 *Pacific Earthquake Engineering Research Invitational Workshop Proceedings, May 14–15, 1998: Defining the Links between Planning, Policy Analysis, Economics and Earthquake Engineering.* Mary Comerio and Peter Gordon. September 1998.

PEER 1998/03 *Repair/Upgrade Procedures for Welded Beam to Column Connections.* James C. Anderson and Xiaojing Duan. May 1998.

PEER 1998/02 *Seismic Evaluation of 196 kV Porcelain Transformer Bushings.* Amir S. Gilani, Juan W. Chavez, Gregory L. Fenves, and Andrew S. Whittaker. May 1998.

PEER 1998/01 *Seismic Performance of Well-Confined Concrete Bridge Columns.* Dawn E. Lehman and Jack P. Moehle. December 2000.